Sensitivity and Uncertainty Analysis for a Fusion-Fission Hybrid System: SOLASE-H

T. Wu and C.W. Maynard

January 1981

UWFDM-401

FUSION TECHNOLOGY INSTITUTE

UNIVERSITY OF WISCONSIN

MADISON WISCONSIN

Sensitivity and Uncertainty Analysis for a Fusion-Fission Hybrid System: SOLASE-H

T. Wu and C.W. Maynard

Fusion Technology Institute
University of Wisconsin
1500 Engineering Drive
Madison, WI 53706

http://fti.neep.wisc.edu

January 1981

UWFDM-401

SENSITIVITY AND UNCERTAINTY ANALYSIS FOR A FUSION-FISSION HYBRID SYSTEM: SOLASE-H[†]

Tang Wu*
and
Charles W. Maynard

Fusion Engineering Program
Nuclear Engineering Department
University of Wisconsin
Madison, Wisconsin 53706

January 1981

UWFDM-401

[†]Research supported in part by the Department of Energy and Wisconsin Electric Utilities Research Foundation

*Present address: General Electric Company, P.O. Box 508, Sunnyvale, California 94086

ABSTRACT

A blankets-coupling one-dimensional model is suggested for the neutronics analysis of the SOLASE-H design. It yields results that are comparable to those of the 3-D Monte Carlo analysis for the fissile production and tritium breeding. The sensitivities of these responses are dominated by the ^{232}Th capture, ^{6}Li (n,α)t, Pb (n,2n), and Pb elastic cross sections. The uncertainties are 6.2% and 3.1% for the fissile production and tritium breeding, respectively.

A. Introduction

The fusion-fission hybrid concept which combines both fission and fusion has been studied extensively by various researchers.[1-5] The coupling utilizes the advantages of both fusion and fission processes. In general, the fission event is considered to be power-rich as 200 MeV is released per fission event compared to 17.6 MeV per D-T fusion. On the other hand, fusion is neutron-rich in the sense that high energy 14.06 MeV D-T neutrons are available for neutron multiplication processes such as (n,2n), (n,3n), and fast fission while fission neutrons average only 2 MeV. The attractiveness of such a hybrid system is therefore due to its ability to produce both fissile fuels and electric power, though the emphasis may lean to one or the other depending upon the design goal of a specific hybrid system. Another factor is that larger energy multiplication enables us to relax the fusion energy requirements. For instance, sub-Lawson plasma confinement parameters in magnetic confinement fusion or low laser/particle beam conversion efficiencies in inertial confinement fusion would be feasible,

which could lead to the introduction of hybrid reactors into the economy earlier than pure fusion devices.

The emphasis on fissile fuel production in a hybrid system leads to the concept of a Fusion Fuel Factory (FFF) discussed by Bethe.[6] Fissile fuels (^{233}U or ^{239}Pu) are produced by neutron capture in the fertile materials (^{232}Th or ^{238}U) for subsequent use in power-generating fission reactors. The main reactions are as follows:

$$^{232}Th(n,\gamma)^{233}Th \xrightarrow[22.2m]{\beta^-} {}^{233}Pa \xrightarrow[27.0d]{\beta^-} {}^{233}U \ ,$$

and

$$^{238}U(n,\gamma)^{239}U \xrightarrow[23.5m]{\beta^-} {}^{239}Np \xrightarrow[2.35d]{\beta^-} {}^{239}Pu.$$

The artificially produced fissile fuels would be used to alleviate the pressure of a supply shortage of ^{235}U, the only naturally-existing fissile isotope. Typical fission reactor fuel assemblies containing natural or depleted materials can be inserted into the hybrid blanket to enrich the fissile concentration to 3-4% before shipping them to the fission reactors for direct use. The aspect of eliminating reprocessing and possible refabrication contributes to tighter proliferation control. It is also possible to make the fuel cladding highly radioactive for safeguard considerations. The linkage between a hybrid reactor as a fissile fuel factory and electricity generating fission reactors has been

discussed by several researchers.[6,7]

In this chapter, the sensitivity and uncertainty analysis for a laser-driven fusion-fission hybrid reactor, SOLASE-H, is presented. The reactor is designed to produce ^{233}U fuel for a typical Light Water Reactor (LWR) fuel assembly. The neutronic design criteria are to have maximum fissile fuel production and to maintain self-sustaining tritium production. ^{232}Th is chosen as the fertile isotope since ^{233}U has better performance in thermal converters. The SOLASE-H blanket studied here is slightly changed from earlier studies[5,8] as a result of a previously unreported optimization study and fulfills the design goals better. Section B presents the blanket description and neutronic analysis which feature an axial-radial blanket coupling model. Sensitivity results are shown in Section C where a description of the difference of sensitivity analysis between pure fusion and fusion-fission hybrid systems is also given. Section D concludes this chapter by presenting the cross section uncertainty analysis.

B. Neutronics Analysis

a. Blanket Description and Calculational Model

The SOLASE-H reactor geometry is shown in Reference 5. The point 14.1 MeV neutron source results from the laser-induced fusion

reactions at the center of a cylindrical cavity of 6 m radius and 12 m height. Three Light Water Reactor (LWR) fuel assemblies, 4 m long, are arranged on top of each other in the radial blanket. An axial blanket located at the top and bottom of the radial blanket is used for both neutron multiplication and tritium breeding. The blanket configuration and materials are slightly different from that of Reference 5 as a result of continuing study by the hybrid research group at the University of Wisconsin.[9] Zircaloy-4 has been chosen as the first wall and structural material and reactor grade graphite is used as the reflector material. Natural lithium is used in this blanket for two main purposes: (1) breeding adequate tritium to make SOLASE-H self-sustaining, and (2) filtering the slow neutrons to reduce the fissioning of the bred ^{233}U. Lead canned in Zircaloy-4 and cooled by sodium is chosen as a neutron multiplier. The thicknesses of the Pb zones immediately following the first wall in the axial and radial blankets are 25 cm and 8.4 cm, respectively. This resulted directly from an optimization study in an effort to maximize the fissile breeding while maintaining tritium breeding around unity.

In the axial direction the blanket consists of a 0.2 cm first wall, 25 cm neutron multiplier zone, 40 cm tritium breeding

zone, 40 cm reflector zone, and another 6.3 cm of tritium breeding material. In the radial blanket, the first wall, 0.2 cm thick, is immediately followed by an 8.4 cm thick neutron multiplier zone, a 2.1 cm Li zone, and then the 21.8 cm thick fissile breeding zone. In the azimuthal direction the fuel assemblies alternate with neutron multiplier zones with a fuel-to-multiplier volume ratio of 1 to enhance the neutron multiplication further. A homogenized mixture of fuel and multiplier will be used in the one-dimensional model. The rest of the blanket following the fuel zone consists of Li (2.1 cm), Pb (8.4 cm), Li (25.2 cm), structural material (2 cm), reflector (30 cm), structural material (2 cm), and Li (6.3 cm). Figure 1 shows the configuration of a coupled one-dimensional model for the SOLASE-H blanket. The material composition and nuclide densities are listed in Table 1.

The blanket neutronics calculation is performed with a P_3- S_4 approximation by the one-dimensional discrete transport code ANISN.[10] A data library with 25 neutron energy groups is prepared from the DLC-41/VITAMIN-C library[11] by use of the AMPX[12] data processing system. The group structure can be found elsewhere.[8] The D-T neutron source is from the laser-pellet interaction in the center of the reactor cavity. The source strength is limited by the radiation damage to the reactor first wall. A 2 MW/m^2 neutron wall loading is chosen for the reactor

cavity of radius 6 m. The total 14 MeV neutron power is therefore $4\pi(6)^2 \cdot 2 = 904.8$ MW, which is equivalent to a neutron source strength of 4.005×10^{20} D-T neutrons/sec.

One-dimensional slab geometry is used in this study. The radial and axial blankets are coupled together to take into account the strong correlation between the two blankets. An anisotropic neutron source which distributes the D-T neutrons by a proportion to the axial and radial blankets with respect to their corresponding solid angles (0.293 and 0.707, respectively) is employed. The ANISN code has been modified to accommodate the angularly dependent distributed source. The reasons for this approach are two-fold. Firstly, it gives a result comparable to that of the three-dimensional Monte Carlo calculations. The simple solid angle weighting approach, in which the 1-D transport calculations are performed for the radial and axial blankets separately and the results weighted by their corresponding solid angles are summed up to obtain the combined result for the system, has been found to have a large discrepancy with respect to the result from the 3-D Monte Carlo calculations. For instance, in an earlier SOLASE-H neutronics analysis, Ragheb et al.[13] find that the simple solid angle weighting model overestimates the fissile breeding by 38% (0.660 vs. 0.479) and underestimates the tritium breeding by 21% (0.881 vs. 1.112). It will be shown later that these discrepancies can be reduced

drastically with the coupled blanket model. Secondly, it would not be possible to evaluate the sensitivity of a response in the radial blanket, for instance, the fissile breeding ratio, to the cross sections of the nuclides in the axial blanket if the decoupled model were used. It is obvious that the blanket coupling technique is essential from the viewpoint of sensitivity and uncertainty analysis.

b. Discussion of Results

Table 2 shows a summary of the neutronics calculations in the SOLASE-H blanket. In this study, we concentrate on two primary responses - the tritium breeding and fissile breeding. Two slightly different blanket systems are studied. One is the fresh fuel system which represents the initial inventory of the PWR fuel assemblies, and the other with 4% of ^{232}Th replaced by ^{233}U.

For the fresh fuel system the fissile breeding ratio is 0.4252 and the tritium breeding ratio is 1.1276 which satisfactorily meets our design criterion of a self-sustaining system in tritium. 98.1% of the tritium production comes from the ^{6}Li (n,t) reaction, although natural lithium is used, due to a softer neutron spectrum resulting from Pb (n,2n) reactions. About 40% of the total tritium production is from the radial blanket. Fast fission of ^{232}Th does not have a great impact on the overall

neutron economy in this system since only 0.018 fission neutrons are produced by thorium per D-T neutron. Neutron multiplication comes mostly from the Pb (n,2n) reactions (0.6177) while the Zr (n,2n) reaction contributes 0.11 neutrons per D-T neutron.

In the previous section, we pointed out the inadequacy of the simple solid angle weighting model and suggested a better model which couples the axial and radial blankets together. In a 3-D Monte Carlo calculation for the same system, the comparable results are 0.434 for the fissile breeding ratio and 1.08 for the tritium breeding ratio.[9] Thus, the 1-D coupled model gives excellent agreement with 3-D Monte Carlo estimates of the fissile and tritium breeding (2.0% and 4.4% difference, respectively). The success of the 1-D coupled model can be understood in that it is able to redistribute the secondary neutrons produced by the Pb (n,2n) reaction in the neutron multiplication zones immediately adjacent to the first wall while the solid angle weighting model fails to do so.

In the system with 4% ^{233}U, the most notable effect is the introduction of 0.2303 neutrons per D-T neutron from the ^{233}U fission reaction. Among those extra fission neutrons, 0.005 and 0.106 neutrons are captured by ^{232}Th and ^{6}Li, respectively, to increase the fissile breeding from 0.425 to 0.430 and the tritium breeding from 1.128 to 1.234. Thus, the presence of the

bred ^{233}U in the fuel assembly has negligible effect as far as the fissile production rate is concerned and only alters the total tritium production slightly. Nevertheless, the ^{233}U absorption reaction, 0.101 per D-T neutron, represents the rate that the bred ^{233}U is being depleted and may be of prime importance in the burnup calculation.

With a fissile breeding ratio of 0.4252 and a source strength of 4.005×10^{20} n/sec, the rate of fissile fuel production would be 1.703×10^{20} ^{233}U atoms/sec, which is equivalent to a yearly ^{233}U production of 2.079 tons. The yearly income on the sale of fissile fuels produced from SOLASE-H, assuming that the average worth of ^{233}U fuel is \$50/gm,[8] is therefore about 104 M\$. Here we only intend to obtain a rough estimate of the income from the sale of the bred ^{233}U fuel. A more detailed economic analysis would have to consider the interest rate, residence time of the fuel assembly, ^{233}U burnup, spatial distribution of the enrichment, technique of rotating the fuel assemblies for achieving a more symmetrically distributed enrichment, initial thorium inventory, etc.

C. Sensitivity Analysis

a. Sensitivity Theory in a Multiplying Medium

Sensitivity theory of a fusion-fission hybrid system differs

from that of a pure fusion system only by the presence of the multiplying medium. In such a system the fission cross sections will influence the calculated results of interest and are usually not negligible. The relative sensitivity function of a response R with respect to a particular cross section Σ at energy E and position r, P(r,E), can be derived from the basic definition, $P = (\Sigma/R)\ (\partial R/\partial \Sigma)$ and the result from first order perturbation theory,[14] i.e.,

$$\delta R \simeq (\phi, \delta \Sigma_r) - (\phi, \delta L^+ \phi^*), \tag{1}$$

where

ϕ, ϕ^* = forward and adjoint angular fluxes,

L^+ = adjoint transport operator,

Σ_r = response function which is also the adjoint source for the adjoint equation,

and (,) represents the integration over the phase space. Upon separating the adjoint transport operator, P(r,E) can be expressed as the sum of four terms. That is,

$$P(r,E) = P_{de}(r,E) + P_{fg}(r,E) + P_{cl}(r,E) + P_{sg}(r,E),$$

where

$P_{de}(r,E)$ = detector term (direct effect)

$$= \frac{\partial \Sigma_r(r,E)}{\partial \Sigma(r,E)} \Sigma(r,E) \int d\Omega \phi(r,E,\Omega)/R, \tag{2}$$

$P_{fg}(r,E)$ = fission gain term

$$= \nu(E)\Sigma_f(r,E)\{\int d\Omega\phi(r,E,\Omega)\}\iint dE'd\Omega'\chi(E')\phi^*(r,E',\Omega')/R, \quad (3)$$

$P_{sg}(r,E)$ = scattering gain term

$$= \sum_{\ell} \frac{2\ell+1}{4\pi} \int dE'\{[\int d\Omega P_\ell(\Omega)\phi(r,E,\Omega)]\,\Sigma_\ell^s(E\to E') [\int d\Omega' P_\ell(\Omega')\phi^*(r,E',\Omega')]\}/R, \quad (4)$$

$P_{cl}(r,E)$ = collision loss term

$$= -\Sigma(r,E)\int d\Omega\phi^*(r,E,\Omega)\phi(r,E,\Omega)/R \quad (5)$$

Note that the detector term exists only if (1) Σ is the response function itself or, (2) any change in Σ will affect the response function (for instance, if ^{6}Li(n,t) is the cross section of interest while the response is total tritium production). Also, notice that there would be no scattering gain term if Σ were an absorption cross section. It is the fission gain term that accounts for the effect of fission cross sections of the fissionable nuclides in a fusion-fission hybrid system.

The cross section sensitivity code SWANLAKE,[15] developed for cross section sensitivity calculation in radiation transport problems, does not have the capability of dealing with the fission process and the response function itself. Some modifications of

SWANLAKE are therefore needed in order to carry out the sensitivity analysis for SOLASE-H. A modified SWANLAKE code is given in the Appendix which also shows the detailed input instructions and output description.

b. Sensitivity of Fissile Breeding and Tritium Breeding

Only two primary responses of SOLASE-H have been investigated here, i.e., fissile breeding and tritium breeding. Table 3 presents the energy-integrated sensitivities with respect to a list of total and partial cross sections for the fresh fuel system of the SOLASE-H blanket, while Table 4 shows the result for the 4% ^{233}U system. All the numbers represent the total effect (sum of direct and indirect effects) summing over all spatial zones. The numbers under the total cross sections must be exactly the sum of partial cross section sensitivities. This peculiar phenomenon, which is caused by the combined effects of the linearity of the transport operator and the first order sensitivity theory and would not be true for higher order theory, can be utilized for checking the consistency of the calculated sensitivity. The partial transfer matrices are generated from the DLC-41/VITAMIN-C data library via the AMPX module NITAWL.

Figures 2 to 17 show a series of sensitivity profiles. These are graphic displays of relative sensitivity per unit lethargy with respect to neutron energy. Solid (dashed) lines

represent negative (positive) sensitivities where the response decreases (increases) as the cross section increases. By visualizing these profiles one can immediately identify, for a particular response, in what energy range a particular cross section type would have the greatest impact. It provides the information by which we are able to pre-select the most important cross section as a function of nuclide, spatial zone, reaction type, and energy range for the uncertainty analysis. Otherwise, the uncertainty analysis would be a very tedious process if all the sensitivity data were to be used for the uncertainty calculation.

For the fresh fuel system the fissile breeding is most sensitive to the cross sections of ^{232}Th, Pb, and ^{6}Li with the total sensitivities of 0.4057, 0.3778, and -0.2208, respectively. Among the partial cross sections of ^{232}Th, the largest sensitivity is from the capture reaction, 0.3545, which has a flux perturbation term of -0.6455 and a direct effect of 1.0 since the capture cross section is the response function itself. Fission cross section and fission yield do not play an important role in this system with sensitivities of 0.0077 and 0.0125, respectively. Sensitivity profiles for the direct effect of the Th (n,γ) cross section merely resemble a detailed energy-dependent fissile production rate which is peaked at about 1 keV. The sensitivity to the lead total cross section is 0.378 where 0.245 and 0.002

comes from zone 14 and zone 10, respectively. It implies that the 8.4 cm Pb zone thickness in the radial blanket is adequate as far as maximizing fissile breeding is concerned. It also suggests that increasing the Pb zone thickness in the axial blanket could still enhance the fissile production due to the fact that Pb (n,2n) neutrons produced in the axial blanket would transport into the radial blanket and therefore contribute to the fissile production. Although the sensitivities from the Pb (n,3n) and inelastic scattering cross sections are small, 0.011 and 0.018, respectively, they are not negligible because of large uncertainties associated with these cross sections and will inevitably have considerable contribution to the fissile breeding uncertainty. The rest of the cross section sensitivities are considerably smaller except in the case of ^{6}Li (n,t) cross section which dominates the lower energy regime with the characteristic 1/v behavior. Incidentally, most of the elastic scattering processes have positive sensitivity in the energy region above 1 keV where the scattering process tends to gradually slow down the high energy neutrons into the ^{232}Th resonance region. In contrast sensitivities are negative because of strong competition from the ^{6}Li (n,t) reaction for the energy region below 1 keV.

For the total tritium production, it was pointed out earlier that ^{6}Li (n,t) and ^{7}Li (n,n')t have a respective contribution of

98.12% and 1.88%. Thus, the direct effects to the sensitivity of the tritium breeding would be 0.9812 and 0.0188 for the ^{6}Li (n,t) and ^{7}Li (n,n')t cross sections, respectively. The sensitivity calculation by the modified SWANLAKE program shows 1.1298 and 0.0188, respectively. The inconsistency for the ^{6}Li arises from the following effects: (1) the ^{6}Li (n,t) cross section is very large in the thermal energy range, (2) the sensitivity calculation uses the boundary angular fluxes instead of scalar fluxes. In a sensitivity calculation, the angular flux for a particular mesh interval is computed by arithmetically averaging the two boundary fluxes directly taken from the discrete transport code, e.g., ANISN. The scalar flux used for calculating the direct effect (Eq. 2) is merely the sum of angular fluxes multiplied by their angular weightings. On the other hand, the response calculated in ANISN uses the interval scalar fluxes directly instead of boundary fluxes. If the variation of the spatial flux distribution is not large, consistent results from the two different approaches are to be expected, as in the cases of fissile breeding and the ^{7}Li (n,n')t reaction. Unfortunately, that is not the case for the ^{6}Li (n,t) reaction where the thermal group contributes considerably and the thermal flux changes drastically across the boundaries separating the Li zone and the other non-Li zones. Consider a mesh interval inside the ^{6}Li zone near a zone boundary. Let N_i, N_{i+1}, and N be the flux levels for the two interval boundaries

and the interval average, respectively. Given N_i and let S, V, A, μ, σ be the source, volume, area, angular weighting, and total cross section, respectively, for slab geometry, then N_{i+1} and N are usually solved by the linear model in conjunction with the diamond-difference model. That is,

$$N_{i+1} = 2N - N_i \ , \tag{6}$$

and

$$N = \frac{SV + 2\mu A\, N_i}{\sigma V + 2\mu A} \ . \tag{7}$$

In the case that σ is large enough to cause a negative N_{i+1}, which is physically meaningless, a step model is instead implemented to have the following expression:

$$N_{i+1} = N = \frac{SV + \mu A\, N_i}{\sigma V + \mu A} \ . \tag{8}$$

Then the interval flux is no longer the arithmatic average of the boundary fluxes and the above-mentioned discrepancy occurs. In the SOLASE-H blanket, the thermal group fluxes change rapidly across the mesh intervals near the L_i zone boundary where the linear model fails. Thus, in these intervals we would find the occurrence of an inconsistency. A simple calculation shows that the difference in the thermal energy region between N and $\frac{1}{2}(N_i + N_{i+1})$ near the Li zone boundary is as high as 80% even when

a 1 cm interval thickness is used. There are two alternatives for remedying the above-mentioned inconsistency: (1) Using the scalar fluxes from ANISN to calculate the direct effect which will lead to a correct direct effect but the total effect would be misleading since the indirect effect is always calculated from the boundary fluxes, (2) Decreasing the mesh size near the Li zone boundary which would give us a consistent set of sensitivity coefficients but the computational effort increases accordingly. The second alternative is recommended if the computing cost is not a major factor.

Table 4 presents the result of sensitivity calculations for the 4% ^{233}U system. No partial cross section sensitivity calculation except for ^{233}U is performed since the sensitivities for the total cross sections are only slightly different from those of the fresh system. As far as the partial cross sections of ^{233}U are concerned, both fissile and tritium breeding are most sensitive to the neutron yields per fission, $\bar{\nu}$, with their respective sensitivities of 0.1585 and 0.1265.

D. Uncertainty Analysis

The uncertainty of a response R, ΔR, defined as the square root of its variance, can be computed from the sensitivity to the data field and the data covariance matrices. A general matrix

representation of ΔR, derived from the statistical error propagation theory, and the first order perturbation theory, has the following form:[16]

$$(\Delta R)^2 = SDS^t, \tag{9}$$

where S is a row matrix representing the sensitivities of R with respect to a set of cross sections, S^t is the transpose of S, and D is the data covariance matrix. In practice, the relative sensitivity matrix P is given from a sensitivity code and a modified form is implemented. That is

$$(\Delta R/R)^2 = P\ \hat{D}\ P^t, \tag{10}$$

where $\hat{D}$ is the relative covariance matrix. Eq. (10) connects the data covariance and sensitivity for estimating the uncertainty of a given response.

During the past few years, some progress has been made at generating a reasonable amount of covariance data for use in the fast reactor program. Unfortunately, there are still only a limited amount of covariance data available for fusion application even with the release of the ENDF/B-V files. In the case that the response is sensitive to a particular cross section and its covariance data cannot be found, one has

to take some educated guesses which would inevitably cause concerns over the accuracy of the uncertainty calculations.

In the SOLASE-H blanket we are fortunate to have uncertainty files available from ENDF/B-V for most of the important cross sections. Covariance matrices for ^{232}Th, ^{16}O, ^{6}Li (< 1 MeV), ^{12}C, Pb and ^{23}Na are processed from the ENDF/B-V uncertainty files by the UNCER code.[17] A set of 10% uncorrelated standard deviations is assumed for ^{7}Li and Zr, due to lack of covariance files, to give a rough estimate of the contribution from these two nuclides. Table 5 shows the reaction MT numbers[18] to be used in this section.

Figures 18 to 24 present a series of graphs resulting from application of the UNCER code. For each reaction type, the correlation matrix is shown on the top half of the figure, while the group cross sections and relative standard deviations, shown in solid and dashed lines, respectively, are in the bottom half. Correlation matrices for different reaction types are also plotted without showing the cross sections and standard deviations. MAT and MT are numbers are designated for nuclide and reaction type, respectively, in the usual ENDF/B convention. Upon looking at these graphs, one can immediately have a clear image of how the basic nuclear data are correlated and what the cross sections and their uncertainties are as a function of energy.

Usually the correlation between two cross section types of different nuclides is possible if the cross section evaluation involves a standard cross section (for instance, ^{235}U fission cross section or ^{10}B (n,α) cross section). Then it would not be practical to identify the contribution to a response uncertainty by a particular nuclide since there exists a so-called cross-MAT term. In our case, no cross-MAT correlation has been found that enables us to break up the total response uncertainty into the sum of contributions from different nuclides. Tables 6 and 7 show the calculational results for the uncertainty of fissile breeding and tritium breeding, respectively.

For the fissile breeding, the total uncertainty from all the nuclides is 6.19%. ^{232}Th cross sections alone contribute 3.89% and Pb cross sections produce 4.67%. Uncertainty due to the rest of the nuclides is negligible. The ^{232}Th (n,γ) cross section has the dominant contribution among all the ^{232}Th partial cross sections due to its large sensitivity. For the Pb partial cross sections, we find that the fissile breeding uncertainty is dominated by inelastic, (n,2n), and (n,3n) cross sections. The large (n,2n) contribution is justifiable because of the large sensitivity. On the other hand, the domination of (n,3n) and total inelastic cross sections is only caused by their unusually large standard deviations in the high energy region (Fig. 21).

These peculiarly large standard deviations occur in the high energy range due to the fact that these cross sections are "derived" from other "evaluated" cross sections (total, elastic, absorption, (n,2n), etc.). Subsequently the covariance matrices for these cross sections are also "derived" from other cross sections. In the process of deriving these covariance matrices in computer programming, some approximations are used and precision might possibly be lost which can lead to the unreasonably large standard deviations. This could be remedied if double precision and a better approximation are implemented.

For tritium breeding, the total uncertainty from all the nuclides is 3.10% where ^{232}Th and Pb cross sections alone contribute 1.10% and 2.75%, respectively. The detailed contributions from the partial cross sections generally tend to have the same trend as those of the fissile breeding uncertainty.

The economic implication of the calculated fissile breeding and tritium breeding uncertainty can not be easily analyzed unless a full scale economic analysis of the SOLASE-H design is performed. Also needed is a more detailed neutronic analysis which should include the burnup calculation, the effect of fuel zone management for a more evenly distributed enrichment, as well as the comparison between 3-D and 1-D models. The economic analysis would then have to include not only the worth of ^{233}U

fuel production but also how these bred fuels would support the LWR's for actual electricity generation. A much simplified analysis is given here.

In an earlier section, it was pointed out that a fissile breeding ratio of 0.4252 corresponds to a yearly income of 104 M$ on the scale of 2.079 tons fissile fuel produced in SOLASE-H. With the fissile breeding uncertainty of 6.19%, exclusively due to data uncertainty, the yearly fissile fuel production is then 2.08 ± 0.13 ton (one standard deviation). Thus, the uncertainty in fissile breeding corresponds to a uncertainty in yearly fuel sale of 6.43 M$, not to mention the economic impact on those power generating LWR's that SOLASE-H would support.

Uncertainty of the tritium production is generally considered of secondary importance as long as the system remains self-sustaining in tritium. A 3.1% uncertainty in tritium breeding should not have any significant impact with the possible exception of designing the tritium handling system.

Uncertainty analysis such as we discussed earlier can be very powerful in identifying where the cross sections should be improved. For instance, the dominant contributions to the fissile production uncertainty for the SOLASE-H blanket are found to be (1) the ^{232}Th (n,γ) in group 21, (2) Pb (n,2n) in group 1, (3) Pb (n,3n) in group 1, (4) Pb total inelastic in group 1, and

(5) Pb total inelastic in group 16. Table 8 shows the standard deviation and sensitivity coefficient of these cross sections. The domination is due to (1) large sensitivity, (2) large data uncertainty, or (3) a combination of (1) and (2). From Table 8 we find that these cross sections alone lead to the fissile breeding uncertainty of 5.5%, which is comparable to 6.2%, the sum over all the nuclides. A thorough examination of the ENDF/B-V uncertainty files reveals, as far as the Pb evaluation is concerned: (1) a 30% uncertainty for the (n,γ) cross section from 10 to 20 MeV, (2) a 5% uncertainty for the nonelastic cross section from 5 to 20 MeV, (3) a 10% uncertainty for the (n,2n) cross section from 12 to 15 MeV, (4) a 15% uncertainty for the inelastic cross section from 14 to 16 MeV, (5) that from 14.179 MeV, the threshold energy, to 20 MeV, the (n,3n) cross section is derived as nonelastic-inelastic - (n,2n) - (n,γ), and (6) from 9 to 14 MeV, the inelastic cross section is derived as nonelastic - (n,2n) - (n,γ). It is the implementation of those "derived" cross sections which usually causes an uncertainty files processor such as UNCER to have some unusually large standard derivations due to the lack of precision in computation. It is therefore suggested that either the uncertainty files evaluator give a direct estimate of data uncertainty instead of those "derived" forms or implement a better uncertainty file processor with superior precision and approximation in order to

obtain more reasonable covariance matrices for the cross sections such as Pb (n,3n) and total inelastic.

If the standard deviations of the Pb (n,3n) and inelastic cross sections are to have a reasonable value, say 20%, one could immediately draw the conclusion that the fissile breeding uncertainty will be dominated by the ^{232}Th (n,γ) and Pb (n,2n) cross sections. Then the target data improvement would be (1) the ^{232}Th (n,γ) cross section around 1 keV and (2) the Pb(n,2n) cross section in the 14 MeV region. This conclusion should be attainable qualitatively even without an uncertainty calculation since (1) the ^{232}Th (n,γ) cross section is the response function itself and (2) the Pb (n,2n) is the major neutron multiplication reaction which induces extra neutrons to improve the neutron economy. Nevertheless, uncertainty analysis does give a quantitative result to the uncertainty of the responses of interest and should provide a basis for quantitative data assessment and, given a set of pre-defined margins on the design parameters, whether or not the calculated response uncertainties are tolerable.

References

1. B.R. Leonard, Nucl. Technol., 20, 161 (1973).

2. L.M. Lidsky, Nucl. Fusion, 15, 151 (1975).

3. J. Maniscalco, Nucl. Technol., 28, 98 (1976).

4. R.W. Conn, G.A. Moses, and S.I. Abdel-Khalik, "Notes on Fusion Hybrid Reactors," UWFDM-240, Fusion Research Program, The University of Wisconsin (1978).

5. R.W. Conn et al., "SOLASE-H, A Laser Fusion Hybrid Reactor Study," UWFDM-270, Fusion Research Program, The University of Wisconsin (1978).

6. H.A. Bethe, "The Fusion Hybrid," Nucl. News, 21, 41 (May 1978).

7. G.A. Moses, R.W. Conn, and S.I. Abdel-Khalik, "Laser Fusion Hybrids-Technical, Economics and Proliferation Considerations," UWFDM-272, Fusion Research Program, The University of Wisconsin (1978).

8. M.M.H. Ragheb et al., "Three-Dimensional Neutronics Analysis of the SOLASE-H Laser Fusion Fissile-Enrichment-Fuel-Factory," UWFDM-266, Fusion Research Program, The University of Wisconsin (1978).

9. M.M.H. Ragheb, Private Communication (1979).

10. W.W. Engle, Jr., "A User's Manual for ANISN," K-1693, Oak Ridge Gaseous Diffusion Plant (1967).

11. RSIC Data Library Collection, DLC-41/VITAMIN-C, Radiation Shielding Information Center, Oak Ridge National Laboratory (1977).

12. N.M. Greene et al., "AMPX: A Modular Code System for Generating Coupled Multigroup Neutron Gamma Libraries from ENDF/B," ORNL/TM-3706, Oak Ridge National Laboratory (1976).

13. Ref. 8, Appendix (1978).

14. D.T. Dudziak, "Cross Section Sensitivity and Uncertainty Analysis for Fusion Reactors (A Review)," LA-UR-78-3219. Los Alamos Scientific Laboratory (1978).

15. D.E. Bartine, E.M. Oblow, and F.R. Mynatt, "SWANLAKE--A Computer Code Utilizing ANISN Radiation Transport Calculations for Cross Section Sensitivity Analysis," ORNL/TM-3809, Oak Ridge National Laboratory (1973).

16. T. Wu and C.W. Maynard, "The Application of Uncertainty Analysis in Conceptual Fusion Reactor Design," Proc. Seminar-Workshop on Theory and Application of Sensitivity and Uncertainty Analysis, August 22-24, 1978, ORNL/RSIC-42, pp. 191-217, Oak Ridge National Laboratory (1978).

17. T. Wu and C.W. Maynard, "UNCER: A University of Wisconsin Version of Uncertainty Files Processor for ENDF/B-V," UWFDM-291, Fusion Research Program, The University of Wisconsin (1978).

18. M.K. Drake, "Data Formats and Procedures for the ENDF Neutron Cross Section Library," Brookhaven National Laboratory Report BNL-50274 (1974).

Table 1

Material Compositions of SOLASE-H Blanket

Code	Material	Composition	Elements	Nuclide Densities (nuclei/ (barn-cm))
A	First Wall and Structural Material	100% v/o Zircaloy-4 98.24 w/o Zr + 1.45 w/o Sn + .21 w/o Fe + .1 w/o Cr	Zr Sn Cr Fe	4.372-2 4.962-4 7.812-5 1.527-4
B	Neutron Multiplication Zones	65.03 v/o Pb + 26.53 v/o Na + 8.44 v/o Zircaloy-4	Pb Na Zr Sn Cr Fe	2.145-2 6.748-3 3.692-3 4.188-5 6.593-6 1.289-5
C	Fissile Breeding Zones	28.10 v/o ThO_2 + 60.28 v/o Na 10.47 v/o Zircaloy-4 + 1.15 v/o Void	Th O Na Zr Sn Cr Fe	6.415-3 1.283-2 1.533-2 4.580-3 5.195-5 8.179-6 1.599-5
D	Tritium Breeding Zones	68.78 v/o natural Li + 23.25 v/o Na + 7.97 v/o Zircaloy-4	^6Li ^7Li Na Zr Sn Cr Fe	2.364-3 2.950-2 5.914-3 3.486-3 3.955-5 6.226-6 1.217-5
E	Reflector Zones	100% Reactor grade Graphite	C	8.373-2

Table 2

Summary of Neutronics Calculations for SOLASE-H Blanket

Reactions	Fresh Fuel			4% ^{233}U		
	Radial	Axial	Total	Radial	Axial	Total
Th (n,γ)			.4252			.4304
^{6}Li (n,α)t	.4457	.6607	1.1064	.5147	.6980	1.2127
^{7}Li (n,n'α)t	.0108	.0104	.0212	.0112	.0103	.0215
Tritium Breeding	.4565	.6711	1.1276	.5259	.7083	1.2342
Neutron Leakage	.0097	.0061	.0158	.0120	.0063	.0183
Pb (n,2n)	.3227	.2950	.6177	.3229	.2950	.6180
Th (n,2n)			.0121			.0118
Fission neutrons from Th			.0181			.0200
Fission neutrons from ^{233}U						.2303
Parasitic absorption			.2327			.2495
^{233}U absorption						.1005

Remark: All numbers are in the unit of reactions/source neutron.

Table 3

Energy-Integrated Relative Sensitivities for SOLASE-H Blanket (Fresh Fuel)

Cross Sections		Fissile Breeding	Tritium Breeding
^{232}Th	total	.4057	-.1073
	fission	.0077	.0053
	capture	.3545	-.1004
	ν	.0125	.0096
	elastic	.0074	-.0036
	inelastic	.0263	-.0121
	n,2n	.0051	.0016
	n,3n	.0047	.0019
Pb	total	.3778	-.1125
	absorption	-.0233	-.0190
	elastic	.2293	-.1155
	inelastic	.0175	-.0532
	n,2n	.1432	.0714
	n,3n	.0110	.0037
^{6}Li	total	-.2208	.1474
	n,t	-.2263	.1503
	elastic	.0056	-.0024
	inelastic	-.0001	-.0004
^{7}Li	total	.0487	-.0023
	absorption	-.0003	-.0009
	elastic	.0485	-.0153
	inelastic	.0005	.0143
	n,2n	.0002	.0003
^{16}O	total	.0858	-.0394
	absorption	-.0030	-.0027
	elastic	.0912	-.0342
	inelastic	-.0024	-.0025
Zr	total	.0347	-.1186
	absorption	-.0790	-.0639
	elastic	.0964	-.0442
	inelastic	-.0023	-.0266
	n,2n	.0196	.0161
^{23}Na	total	.1478	-.1706
	absorption	-.0546	-.0432
	elastic	.2007	-.0864
	inelastic	.0005	-.0412
	n,2n	.0010	.0001

Table 4

Energy-Integrated Relative Sensitivities for SOLASE-H Blanket (4% ^{233}U)

Cross Sections	Fissile Breeding	Tritium Breeding
^{232}Th total	.4272	-.1404
Pb total	.4016	-.0897
^{6}Li total	-.2370	.1314
^{7}Li total	.0537	-.0017
^{12}C total	.0001	.0386
Zr total	.0428	-.1165
^{23}Na total	.1598	-.1622
^{16}O total	.0926	-.0363
^{233}U total	.0335	.0876
fission	.0446	.0914
ν	.1585	.1265
capture	-.0125	-.0034
elastic	.0003	-.0001
inelastic	.0009	-.0003
n,2n	.0001	.0000
n,3n	.0000	.0000

Table 5

Definition of Reaction MT Numbers

MT Number	Cross Sections
1	total
2	elastic
3	non-elastic
4	total inelastic
16	n,2n
17	n,3n
18	fission
101	absorption
102	n,γ
103	n,P
104	n,d
105	n,t
106	n,^{3}He
107	n,α
452	$\bar{\nu}$, average neutron yield per fission event

Table 6

Uncertainty of Fissile Breeding Ratio ($(\Delta R/R)^2$) Contributed from Different Nuclides in SOLASE-H Blanket

(a) ^{232}Th

MT	18	102	452
18	3.566-3	-	-
102	-	1.509+1	-
452	-	-	1.157-4
sum = 1.509+1, $\Delta R/R$ = 3.885%			

(b) ^{16}O

MT	2	4	101
2	1.484-2	4.054-5	-8.325-7
4	4.025-5	1.243-3	-3.507-4
101	-8.870-7	-3.510-4	1.172-3
sum = 1.663-2, $\Delta R/R$ = 0.129%			

(c) ^{6}Li

MT	2	105
2	3.871-4	-
105	-	2.440-2
sum = 2.479-2, $\Delta R/R$ = 0.157%		

(d) ^{12}C

MT	2	101
2	4.506-7	-
101	-	2.652-7
sum = 7.158-7, $\Delta R/R$ = 0.001%		

(e) Pb

MT	2	4	16	17	101
2	3.722-1	-	-	-	-
4	-	2.929+0	1.727+0	1.235-1	-5.730-7
16	-	1.729+0	1.758+0	-5.149+0	-
17	-	1.235-1	-5.149+0	2.334+1	1.596-6
101	-	-5.747-7	-	1.596-6	1.729-2
sum = 2.182 + 1, $\Delta R/R$ = 4.671%					

(f) ^{23}Na

MT	2	4	101
2	3.509-1	-	1.080-3
4	-	2.733-1	-
101	1.5003-3	-	2.724-1
sum = 8.993-1, $\Delta R/R$ = 0.948%			

(g) ^{7}Li

MT	1
1	1.003-1
$\Delta R/R$=0.317%	

(h) Zr

MT	1
1	3.660-1
$\Delta R/R$=0.605%	

Sum over all nuclides = 3.832+1, $\Delta R/R$ = 6.190%

Table 7

Uncertainty of Tritium Breeding Ratio ($(\Delta R/R)^2$) Contributed from Different Nuclides in SOLASE-H Blanket

(a) ^{232}Th

MT	18	102	452
18	1.675-3	-	-
102	-	1.205+0	-
452	-	-	6.855-5
sum = 1.207+0, $\Delta R/R$ = 1.098%			

(b) ^{16}O

MT	2	4	101
2	2.102-3	-5.694-5	-1.210-6
4	-5.703-5	1.418-3	-3.478-4
101	-1.240-6	-3.483-4	1.007-3
sum = 3.715-3, $\Delta R/R$ = 0.061%			

(c) ^{6}Li

MT	2	105
2	8.119-5	-
105	-	1.076-2
sum = 1.084-2, $\Delta R/R$ = 0.104%		

(d) ^{12}C

MT	2	101
2	1.389-4	-
101	-	6.923-4
sum = 8.312-4, $\Delta R/R$ = 0.029%		

(e) Pb

MT	2	4	16	17	101
2	8.903-2	-	-	-	-
4	-	3.887+0	1.054+0	5.180-2	-7.847-7
16	-	1.055+0	4.222-1	-8.485-1	-
17	-	5.180-2	-8.485-1	2.655+0	5.895-7
101	-	-7.869-7	-	5.895-7	1.239-2
sum = 7.581+0, $\Delta R/R$ = 2.753%					

(f) ^{23}Na

MT	2	4	101
2	6.525-2	-	-1.203-3
4	-	2.483-1	-
101	-1.318-3	-	2.425-1
sum = 5.535-1, $\Delta R/R$ = 0.744%			

(g) ^{7}Li

MT	1
1	2.870-2
$\Delta R/R$ = 0.169%	

(h) Zr

MT	1
1	1.922-1
$\Delta R/R$ = 0.438%	

Sum over all nuclides = 9.578+0 $\Delta R/R$ = 3.095%

Table 8

Major Contributions to Fissile Fuel Production Uncertainty

Cross Section	Group	Energy Range	Standard Deviation (%)	Sensitivity	$\Delta R/R$ (%)
^{232}Th (n,γ)	21	0.35 - 3.35 keV	11.2	0.140	1.568
Pb (n,2n)	1	13.5-14.9 MeV	10.0	0.125	1.250
Pb (n,3n)	1	13.5 - 14.9 MeV	440.0	0.0110	4.840
Pb inelastic	1	13.5 - 14.9 MeV	71.9	-0.0205	1.474
Pb inelastic	16	0.74 - 1.35 MeV	25.4	0.213	0.541

SUM $\left(\sqrt{(\Delta R/R)^2}\right)$ = 5.469%

	Zone Number	Material Code	Thickness (cm)	Number of Mesh Intervals
Radial Blanket	1	D	6.3	3
	2	A	2.0	1
	3	E	30.0	15
	4	A	2.0	1
	5	D	25.2	12
	6	B	8.4	8
	7	D	2.1	2
	8	C+B*	21.8	22
	9	D	2.1	2
	10	B	8.4	4
	11	A	0.2	1
	12	SOURCE		
Axial Blanket	13	A	0.2	1
	14	B	25.0	25
	15	D	40.0	40
	16	E	40.0	20
	17	D	6.3	4

* 50 v/o material C + 50 v/o material B

Fig. 1 Configuration of a One-dimensional Coupled Blanket Model for SOLASE-H.

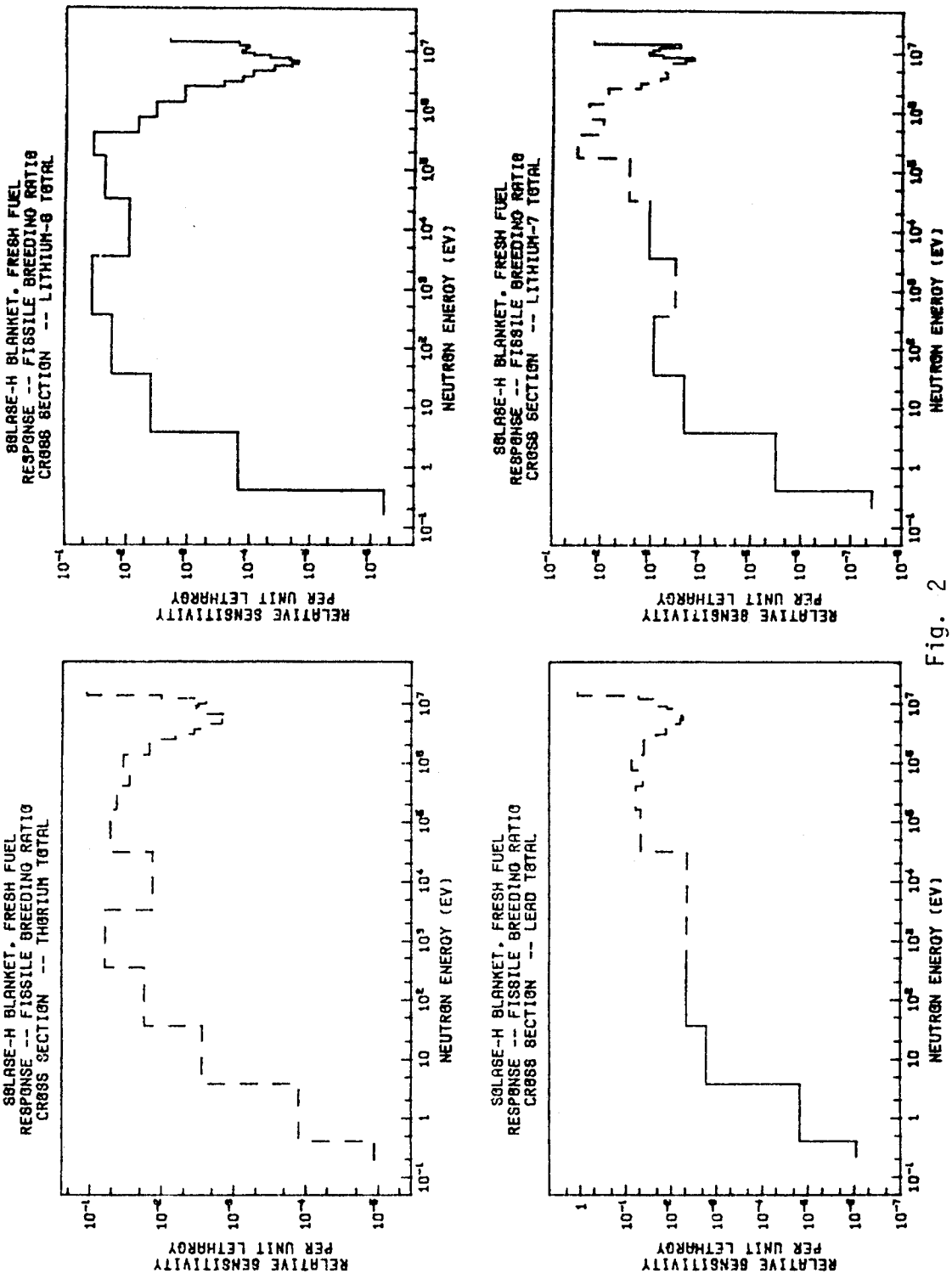
SGLASE-H BLANKET, FRESH FUEL
RESPONSE -- FISSILE BREEDING RATIO
CROSS SECTION -- LITHIUM-6 TOTAL
SGLASE-H BLANKET, FRESH FUEL
RESPONSE -- FISSILE BREEDING RATIO
CROSS SECTION -- LITHIUM-7 TOTAL
SGLASE-H BLANKET, FRESH FUEL
RESPONSE -- FISSILE BREEDING RATIO
CROSS SECTION -- THORIUM TOTAL
SGLASE-H BLANKET, FRESH FUEL
RESPONSE -- FISSILE BREEDING RATIO
CROSS SECTION -- LEAD TOTAL
RELATIVE SENSITIVITY PER UNIT LETHARGY
NEUTRON ENERGY (EV)

Fig. 2

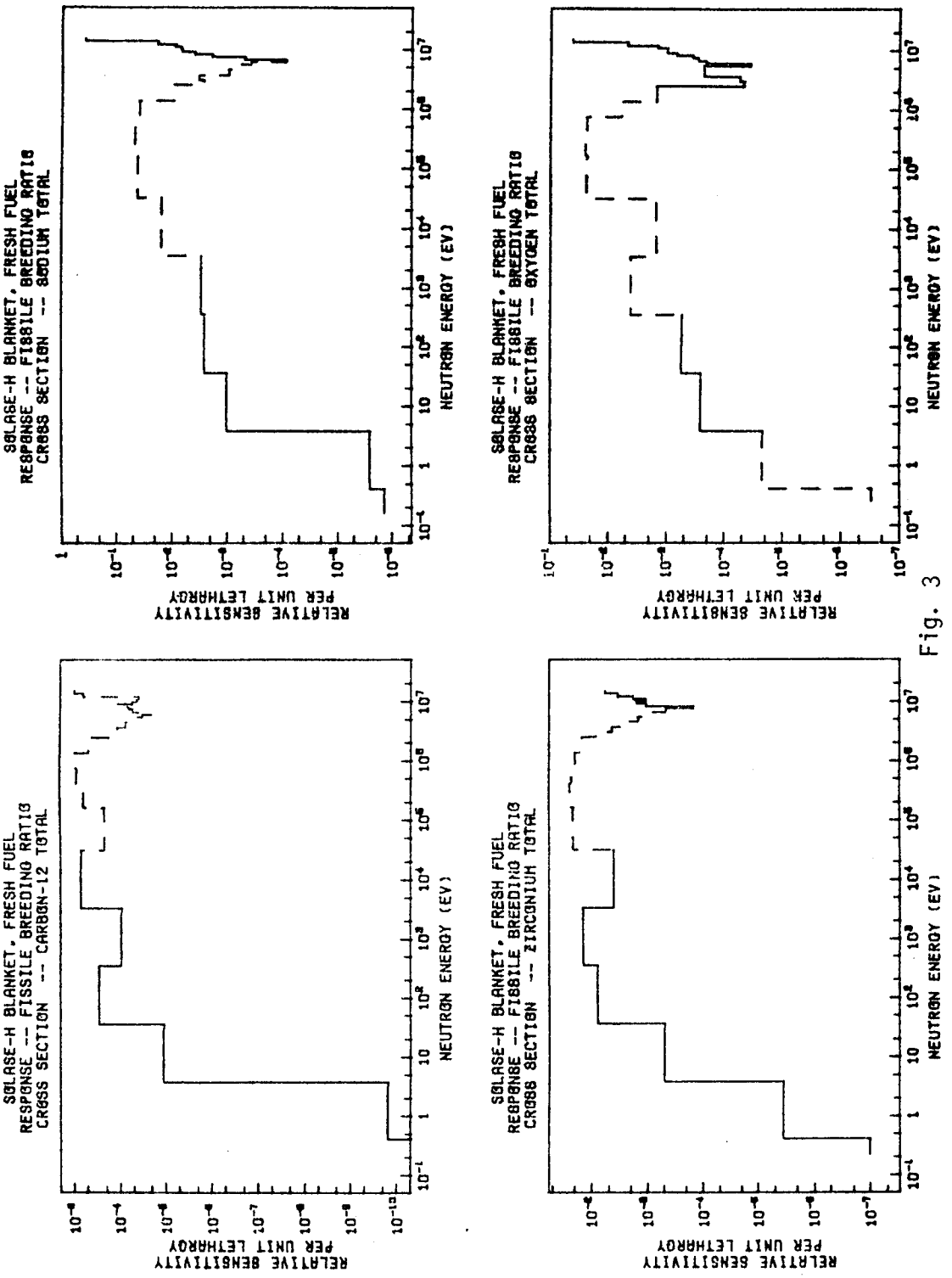
SOLASE-H BLANKET, FRESH FUEL
RESPONSE -- FISSILE BREEDING RATIO
CROSS SECTION -- SODIUM TOTAL
SOLASE-H BLANKET, FRESH FUEL
RESPONSE -- FISSILE BREEDING RATIO
CROSS SECTION -- OXYGEN TOTAL
SOLASE-H BLANKET, FRESH FUEL
RESPONSE -- FISSILE BREEDING RATIO
CROSS SECTION -- CARBON-12 TOTAL
SOLASE-H BLANKET, FRESH FUEL
RESPONSE -- FISSILE BREEDING RATIO
CROSS SECTION -- ZIRCONIUM TOTAL
RELATIVE SENSITIVITY PER UNIT LETHARGY
NEUTRON ENERGY (EV)

Fig. 3

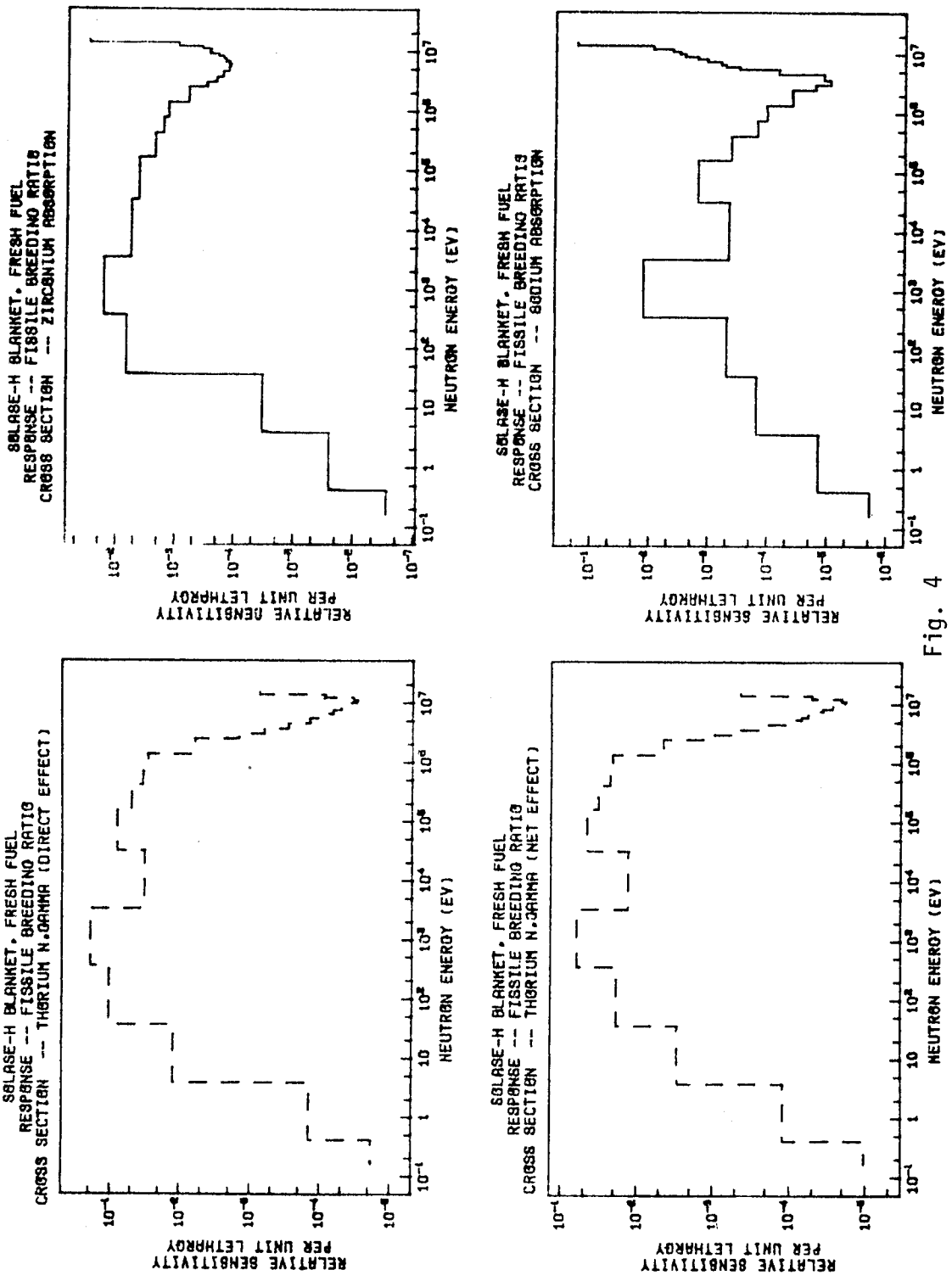
SOLASE-H BLANKET, FRESH FUEL
RESPONSE -- FISSILE BREEDING RATIO
CROSS SECTION -- ZIRCONIUM ABSORPTION
SOLASE-H BLANKET, FRESH FUEL
RESPONSE -- FISSILE BREEDING RATIO
CROSS SECTION -- SODIUM ABSORPTION
SOLASE-H BLANKET, FRESH FUEL
RESPONSE -- FISSILE BREEDING RATIO
CROSS SECTION -- THORIUM N,GAMMA (DIRECT EFFECT)
SOLASE-H BLANKET, FRESH FUEL
RESPONSE -- FISSILE BREEDING RATIO
CROSS SECTION -- THORIUM N,GAMMA (NET EFFECT)
RELATIVE SENSITIVITY PER UNIT LETHARGY
NEUTRON ENERGY (EV)

Fig. 4

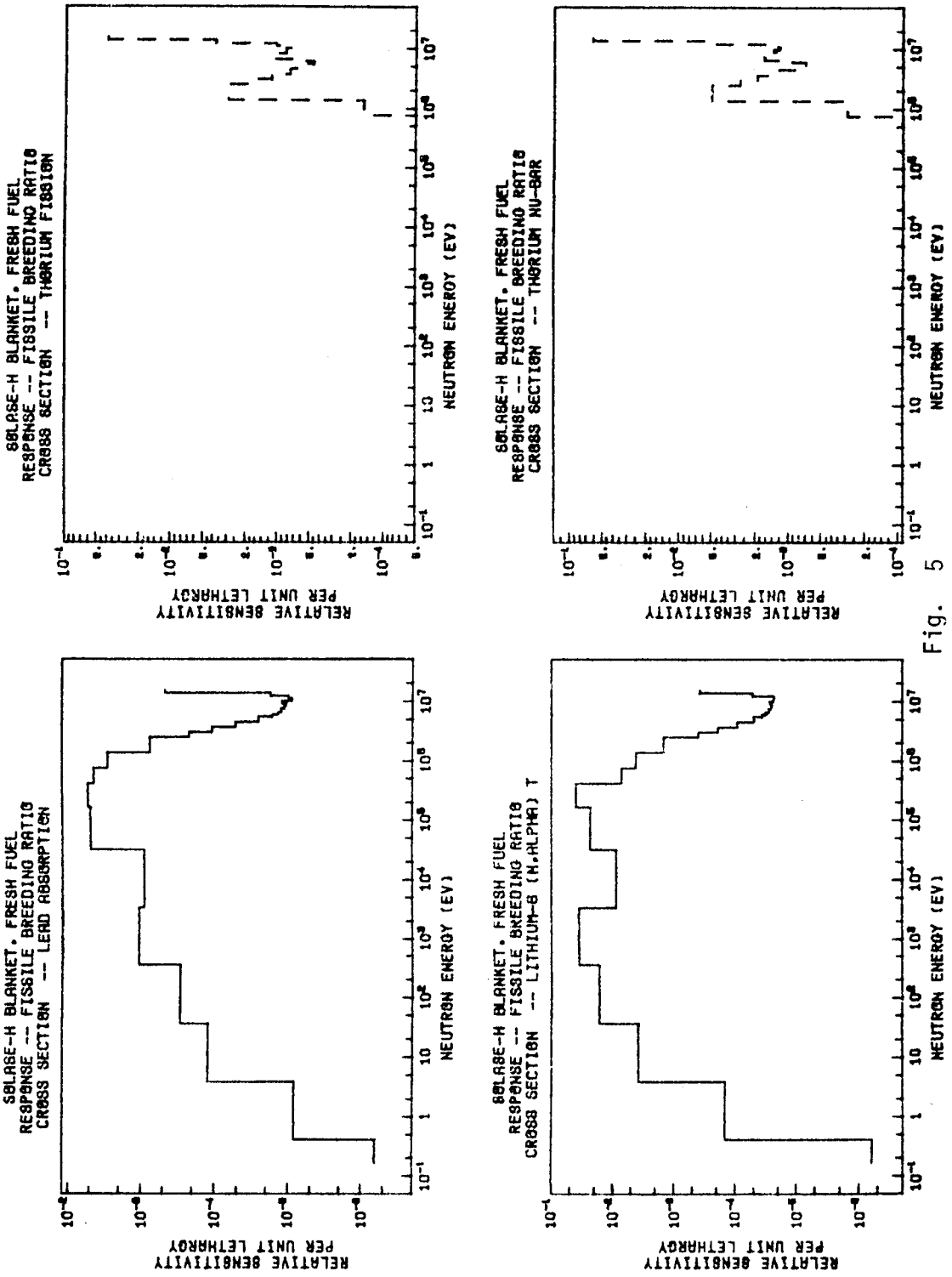
SOLASE-H BLANKET, FRESH FUEL
RESPONSE -- FISSILE BREEDING RATIO
CROSS SECTION -- THORIUM FISSION
SOLASE-H BLANKET, FRESH FUEL
RESPONSE -- FISSILE BREEDING RATIO
CROSS SECTION -- THORIUM NU-BAR
SOLASE-H BLANKET, FRESH FUEL
RESPONSE -- FISSILE BREEDING RATIO
CROSS SECTION -- LEAD ABSORPTION
SOLASE-H BLANKET, FRESH FUEL
RESPONSE -- FISSILE BREEDING RATIO
CROSS SECTION -- LITHIUM-6 (N,ALPHA) T
RELATIVE SENSITIVITY PER UNIT LETHARGY
NEUTRON ENERGY (EV)

Fig. 5

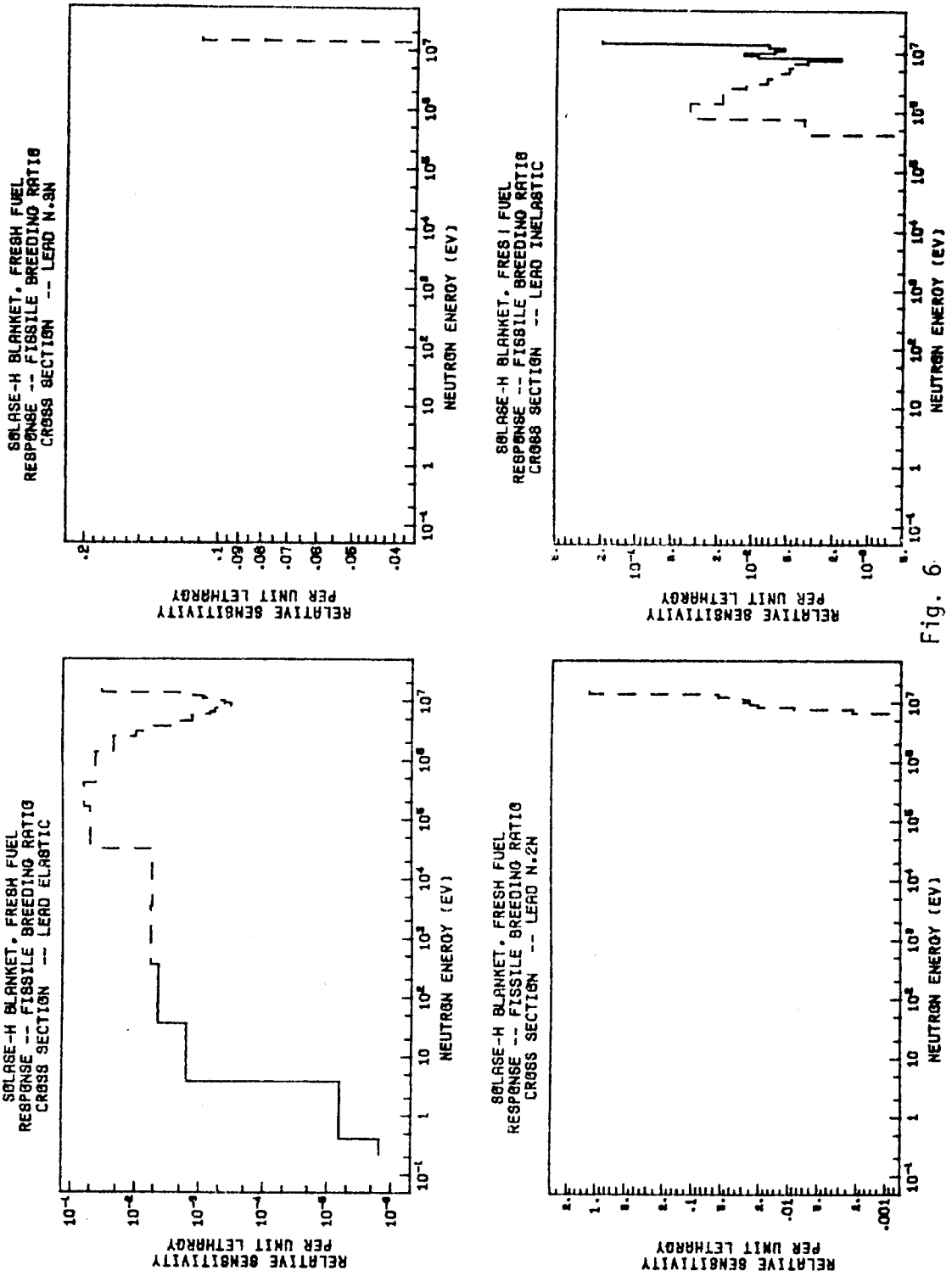
SOLASE-H BLANKET, FRESH FUEL
RESPONSE -- FISSILE BREEDING RATIO
CROSS SECTION -- LEAD N.3N
RELATIVE SENSITIVITY PER UNIT LETHARGY
NEUTRON ENERGY (EV)
SOLASE-H BLANKET, FRES.I FUEL
RESPONSE -- FISSILE BREEDING RATIO
CROSS SECTION -- LEAD INELASTIC
RELATIVE SENSITIVITY PER UNIT LETHARGY
NEUTRON ENERGY (EV)
SOLASE-H BLANKET, FRESH FUEL
RESPONSE -- FISSILE BREEDING RATIO
CROSS SECTION -- LEAD ELASTIC
RELATIVE SENSITIVITY PER UNIT LETHARGY
NEUTRON ENERGY (EV)
SOLASE-H BLANKET, FRESH FUEL
RESPONSE -- FISSILE BREEDING RATIO
CROSS SECTION -- LEAD N.2N
RELATIVE SENSITIVITY PER UNIT LETHARGY
NEUTRON ENERGY (EV)

Fig. 6

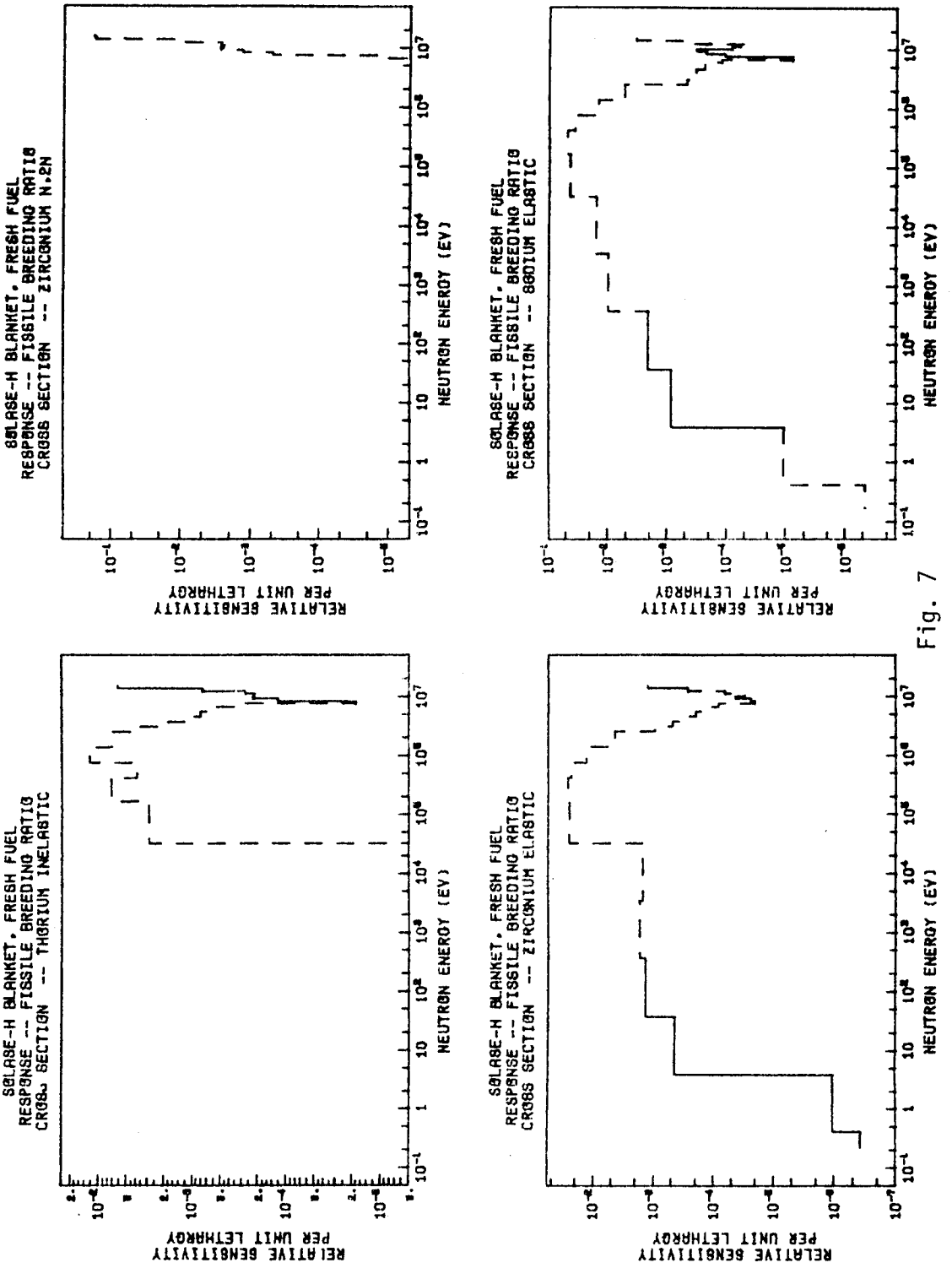
SOLASE-H BLANKET, FRESH FUEL
RESPONSE -- FISSILE BREEDING RATIO
CROSS SECTION -- ZIRCONIUM N,2N
SOLASE-H BLANKET, FRESH FUEL
RESPONSE -- FISSILE BREEDING RATIO
CROSS SECTION -- SODIUM ELASTIC
SOLASE-H BLANKET, FRESH FUEL
RESPONSE -- FISSILE BREEDING RATIO
CROSS SECTION -- THORIUM INELASTIC
SOLASE-H BLANKET, FRESH FUEL
RESPONSE -- FISSILE BREEDING RATIO
CROSS SECTION -- ZIRCONIUM ELASTIC
RELATIVE SENSITIVITY PER UNIT LETHARGY
NEUTRON ENERGY (EV)

Fig. 7

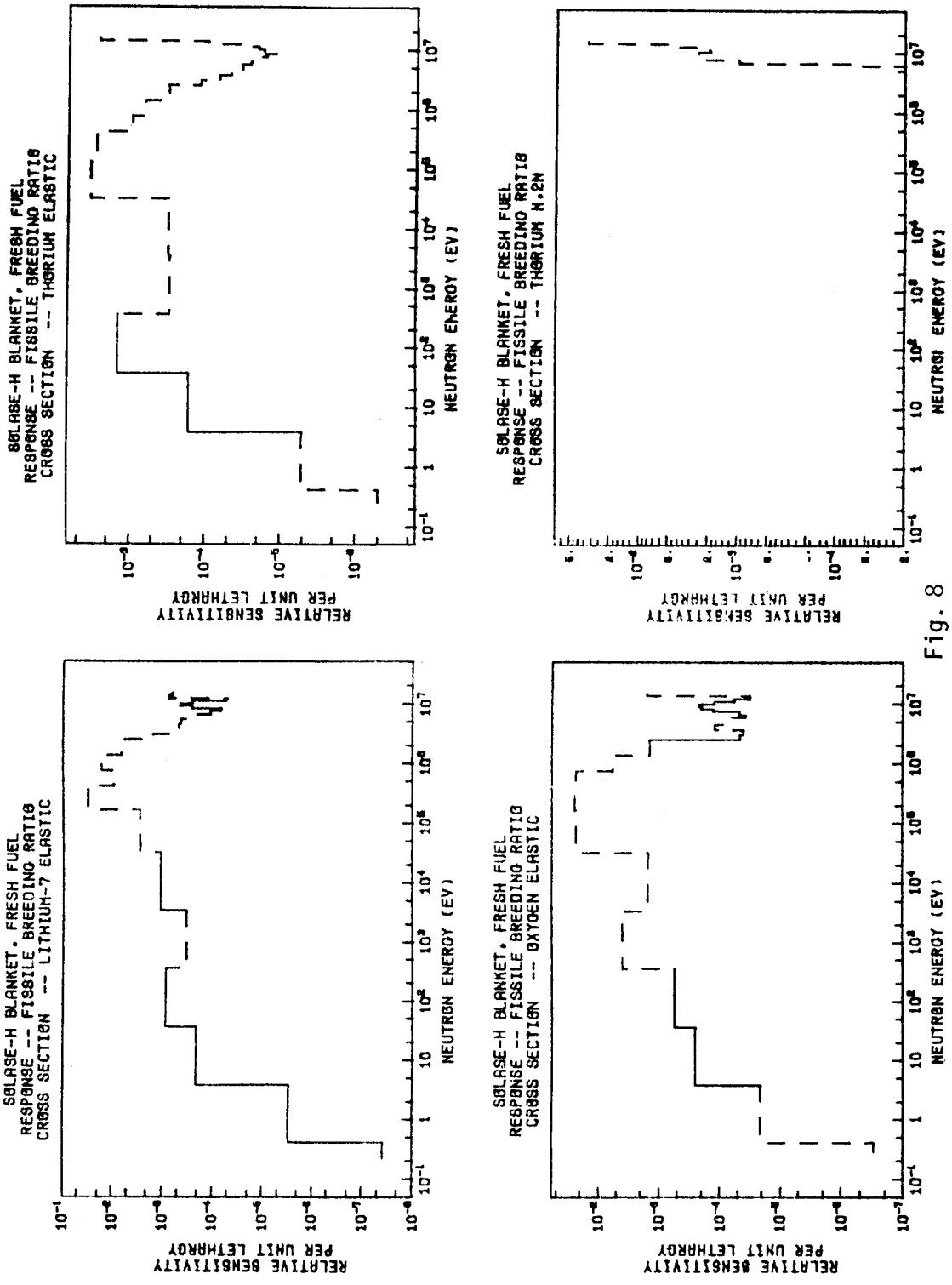
SBLASE-H BLANKET, FRESH FUEL
RESPONSE -- FISSILE BREEDING RATIO
CROSS SECTION -- THORIUM ELASTIC
RELATIVE SENSITIVITY PER UNIT LETHARGY
NEUTRON ENERGY (EV)
SBLASE-H BLANKET, FRESH FUEL
RESPONSE -- FISSILE BREEDING RATIO
CROSS SECTION -- THORIUM N,2N
RELATIVE SENSITIVITY PER UNIT LETHARGY
NEUTRON ENERGY (EV)
SBLASE-H BLANKET, FRESH FUEL
RESPONSE -- FISSILE BREEDING RATIO
CROSS SECTION -- LITHIUM-7 ELASTIC
RELATIVE SENSITIVITY PER UNIT LETHARGY
NEUTRON ENERGY (EV)
SBLASE-H BLANKET, FRESH FUEL
RESPONSE -- FISSILE BREEDING RATIO
CROSS SECTION -- OXYGEN ELASTIC
RELATIVE SENSITIVITY PER UNIT LETHARGY
NEUTRON ENERGY (EV)

Fig. 8

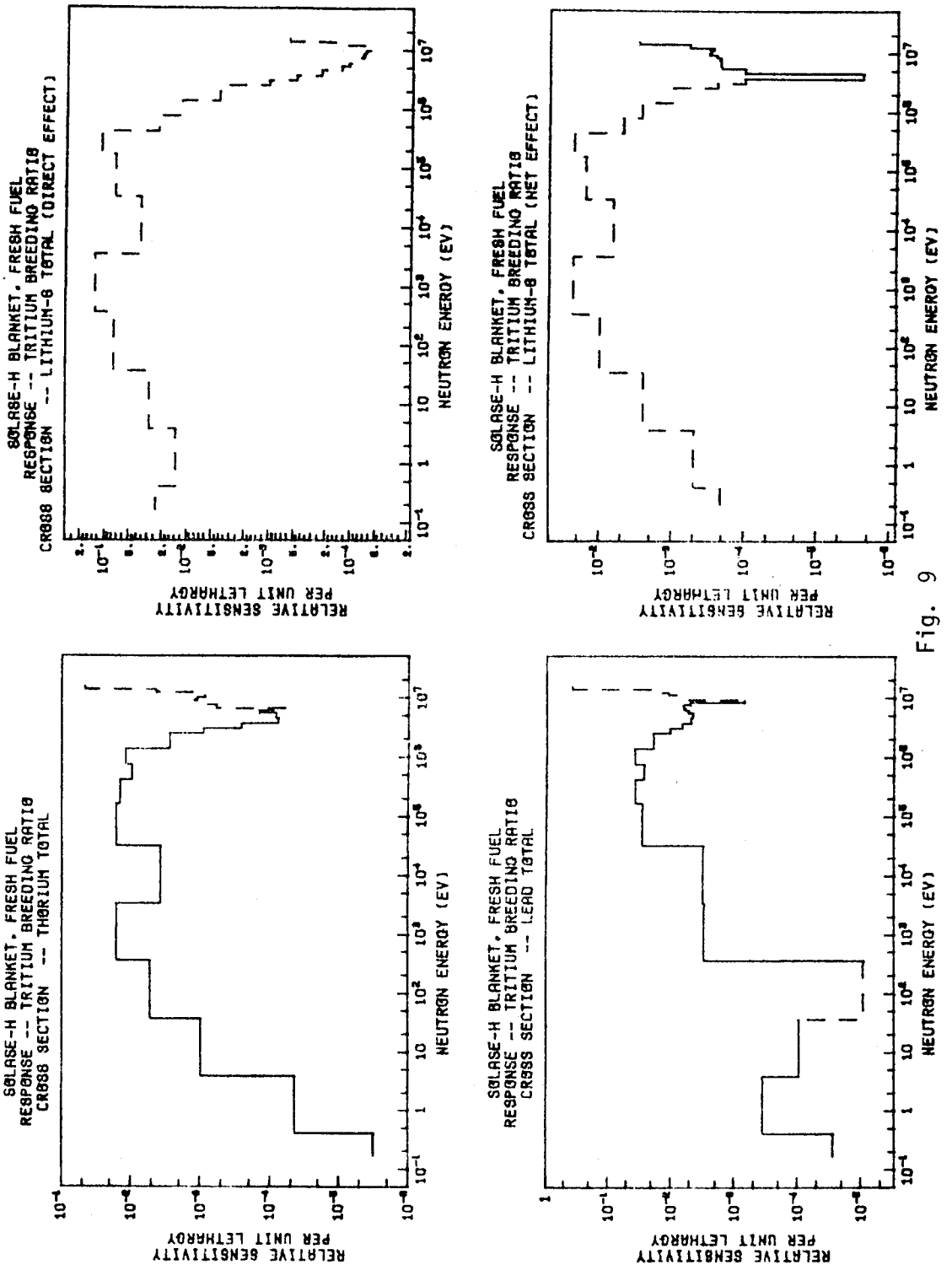
SGLASE-H BLANKET, FRESH FUEL
RESPONSE -- TRITIUM BREEDING RATIO
CROSS SECTION -- LITHIUM-6 TOTAL (DIRECT EFFECT)
SGLASE-H BLANKET, FRESH FUEL
RESPONSE -- TRITIUM BREEDING RATIO
CROSS SECTION -- LITHIUM-6 TOTAL (NET EFFECT)
SGLASE-H BLANKET, FRESH FUEL
RESPONSE -- TRITIUM BREEDING RATIO
CROSS SECTION -- THORIUM TOTAL
SGLASE-H BLANKET, FRESH FUEL
RESPONSE -- TRITIUM BREEDING RATIO
CROSS SECTION -- LEAD TOTAL
RELATIVE SENSITIVITY PER UNIT LETHARGY
NEUTRON ENERGY (EV)

Fig. 9

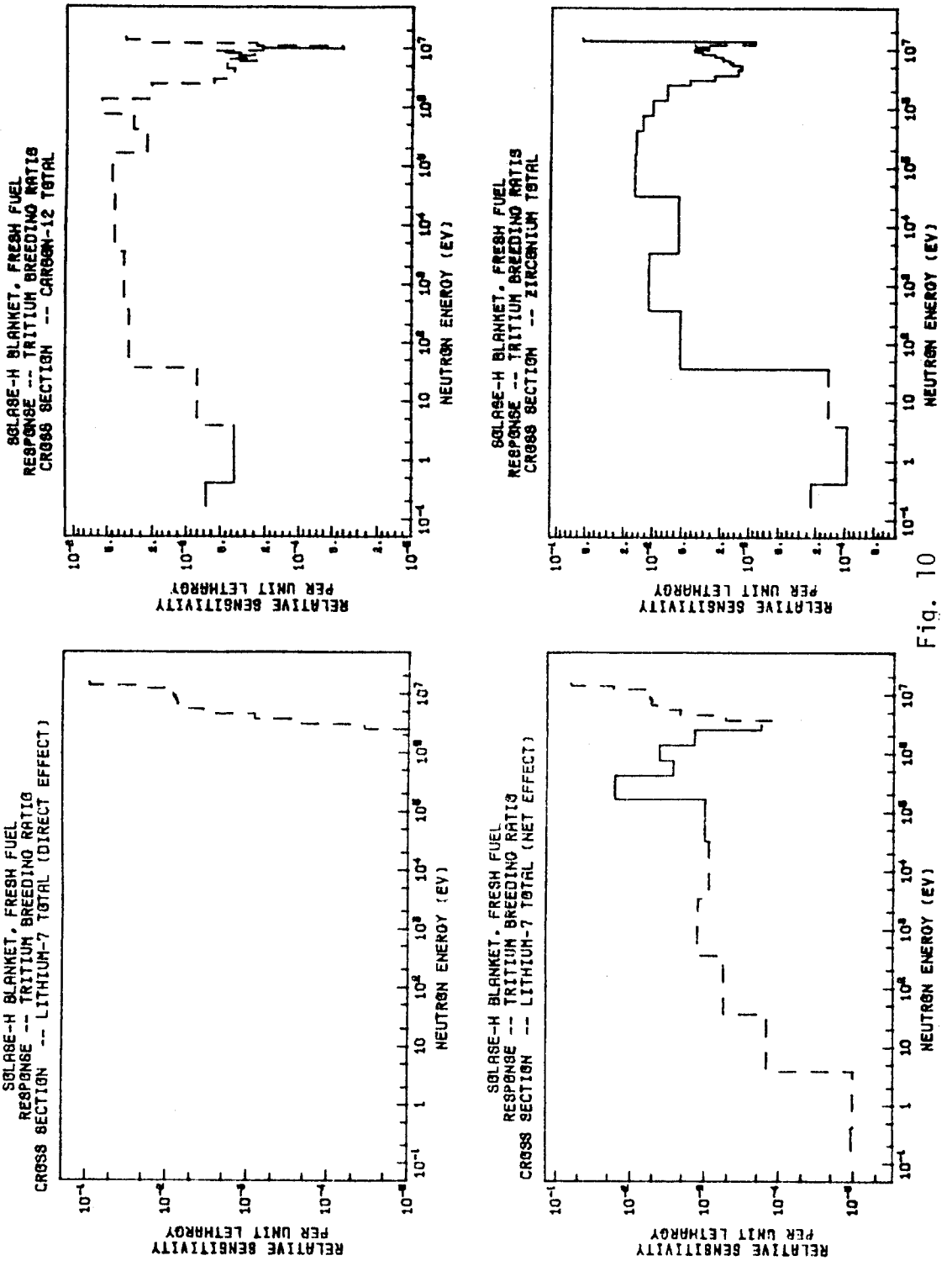
SOLASE-H BLANKET, FRESH FUEL
RESPONSE -- TRITIUM BREEDING RATIO
CROSS SECTION -- CARBON-12 TOTAL
SOLASE-H BLANKET, FRESH FUEL
RESPONSE -- TRITIUM BREEDING RATIO
CROSS SECTION -- ZIRCONIUM TOTAL
SOLASE-H BLANKET, FRESH FUEL
RESPONSE -- TRITIUM BREEDING RATIO
CROSS SECTION -- LITHIUM-7 TOTAL (DIRECT EFFECT)
SOLASE-H BLANKET, FRESH FUEL
RESPONSE -- TRITIUM BREEDING RATIO
CROSS SECTION -- LITHIUM-7 TOTAL (NET EFFECT)
RELATIVE SENSITIVITY PER UNIT LETHARGY
NEUTRON ENERGY (EV)

Fig. 10

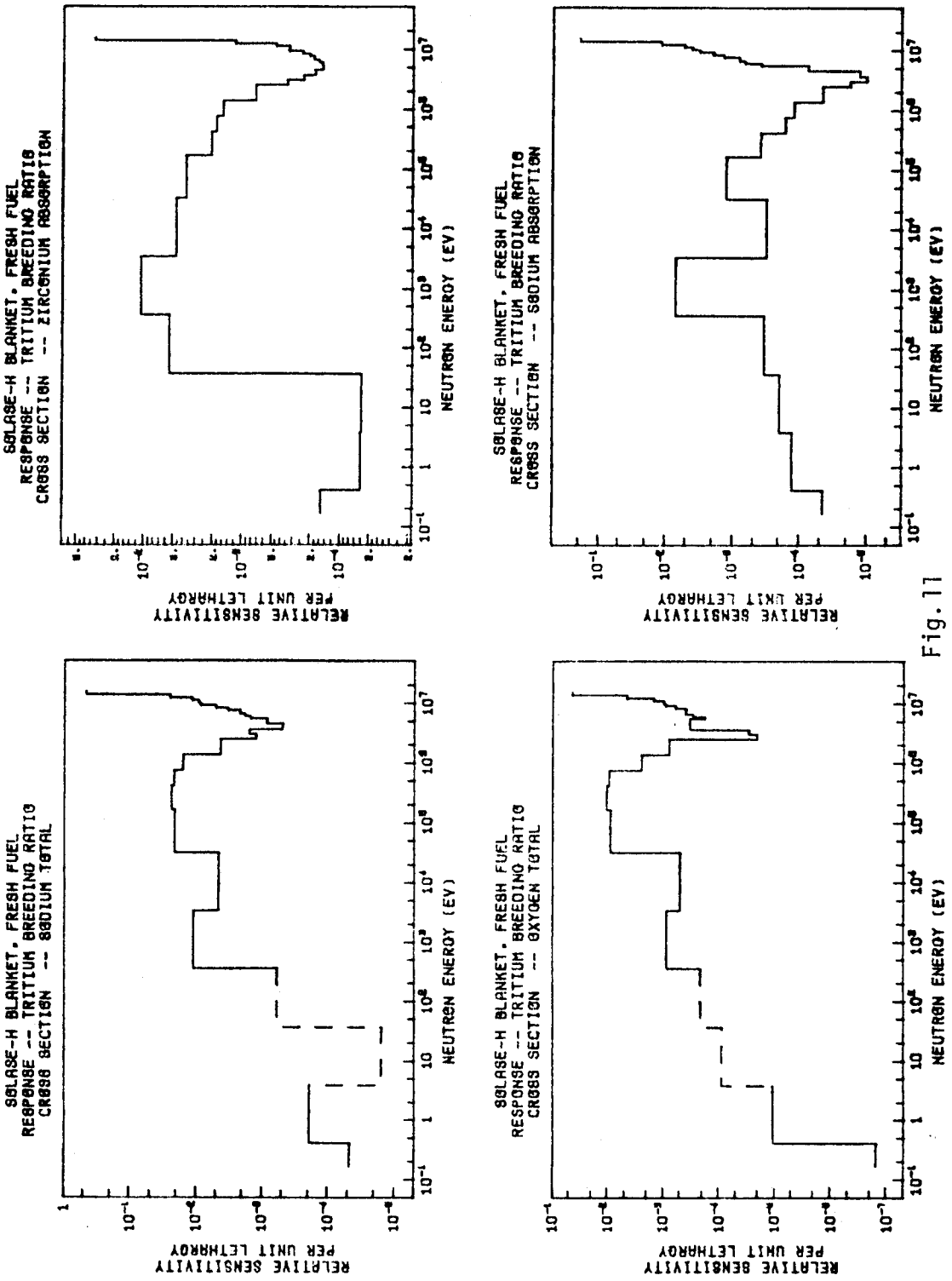
SOLASE-H BLANKET, FRESH FUEL
RESPONSE -- TRITIUM BREEDING RATIO
CROSS SECTION -- ZIRCONIUM ABSORPTION
SOLASE-H BLANKET, FRESH FUEL
RESPONSE -- TRITIUM BREEDING RATIO
CROSS SECTION -- SODIUM ABSORPTION
SOLASE-H BLANKET, FRESH FUEL
RESPONSE -- TRITIUM BREEDING RATIO
CROSS SECTION -- SODIUM TOTAL
SOLASE-H BLANKET, FRESH FUEL
RESPONSE -- TRITIUM BREEDING RATIO
CROSS SECTION -- OXYGEN TOTAL
RELATIVE SENSITIVITY PER UNIT LETHARGY
NEUTRON ENERGY (EV)

Fig. 11

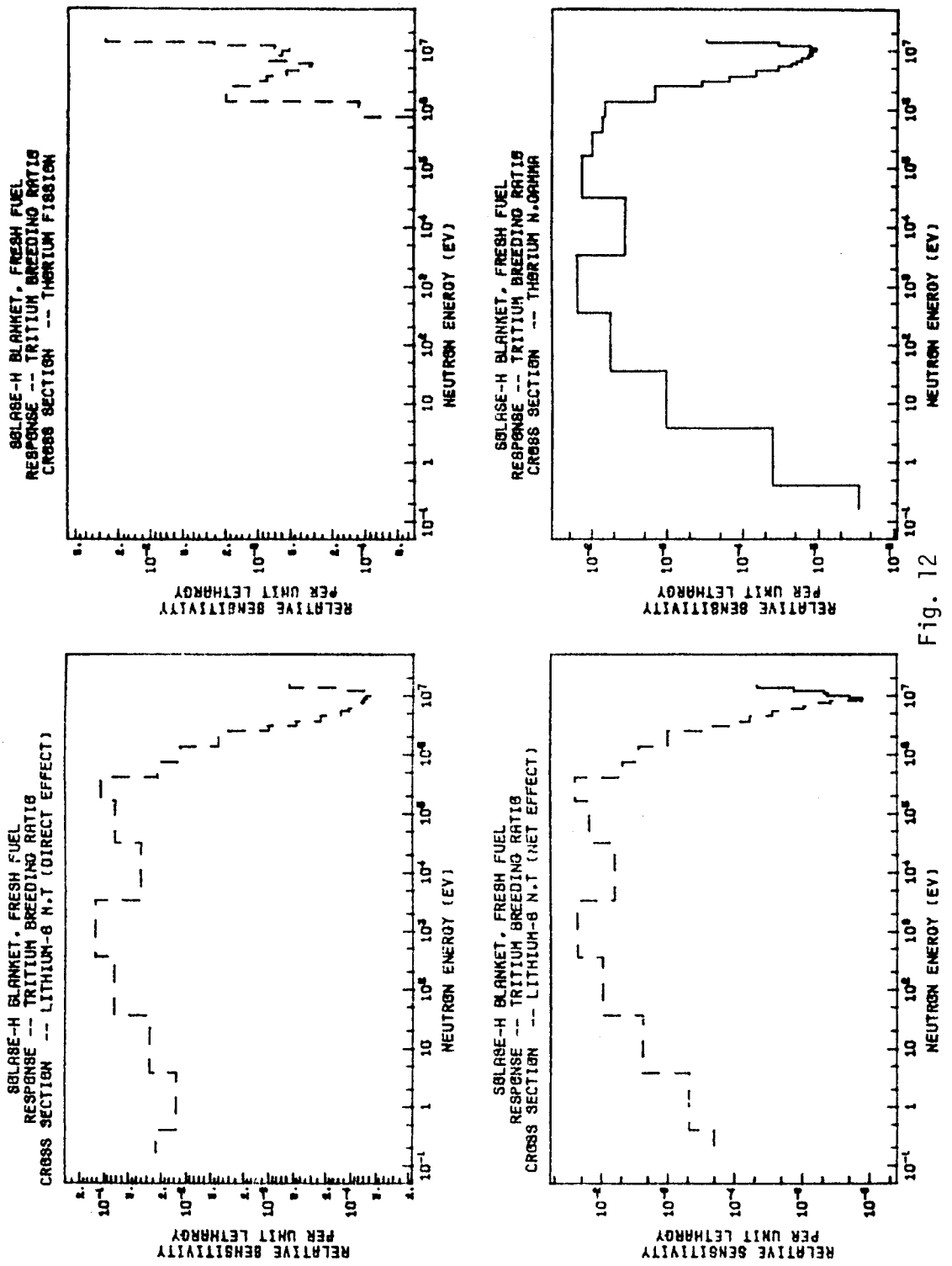
SOLASE-H BLANKET, FRESH FUEL
RESPONSE -- TRITIUM BREEDING RATIO
CROSS SECTION -- THORIUM FISSION
SOLASE-H BLANKET, FRESH FUEL
RESPONSE -- TRITIUM BREEDING RATIO
CROSS SECTION -- THORIUM N,GAMMA
SOLASE-H BLANKET, FRESH FUEL
RESPONSE -- TRITIUM BREEDING RATIO
CROSS SECTION -- LITHIUM-6 N,T (DIRECT EFFECT)
SOLASE-H BLANKET, FRESH FUEL
RESPONSE -- TRITIUM BREEDING RATIO
CROSS SECTION -- LITHIUM-6 N,T (NET EFFECT)
RELATIVE SENSITIVITY PER UNIT LETHARGY
NEUTRON ENERGY (EV)

Fig. 12

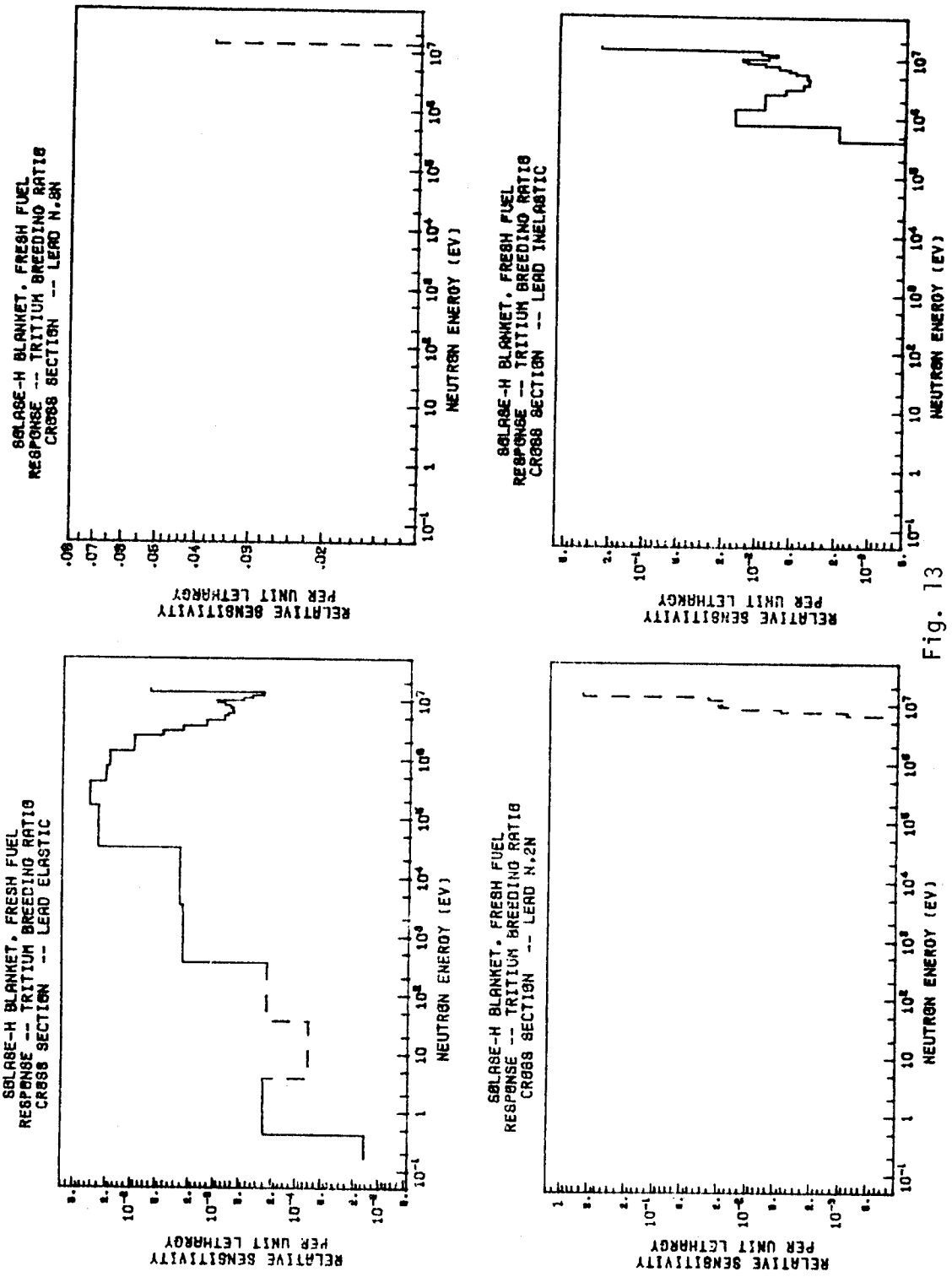
SOLASE-H BLANKET, FRESH FUEL
RESPONSE -- TRITIUM BREEDING RATIO
CROSS SECTION -- LEAD N,2N
SOLASE-H BLANKET, FRESH FUEL
RESPONSE -- TRITIUM BREEDING RATIO
CROSS SECTION -- LEAD INELASTIC
SOLASE-H BLANKET, FRESH FUEL
RESPONSE -- TRITIUM BREEDING RATIO
CROSS SECTION -- LEAD ELASTIC
SOLASE-H BLANKET, FRESH FUEL
RESPONSE -- TRITIUM BREEDING RATIO
CROSS SECTION -- LEAD N,8N
NEUTRON ENERGY (EV)
RELATIVE SENSITIVITY
PER UNIT LETHARGY

Fig. 13

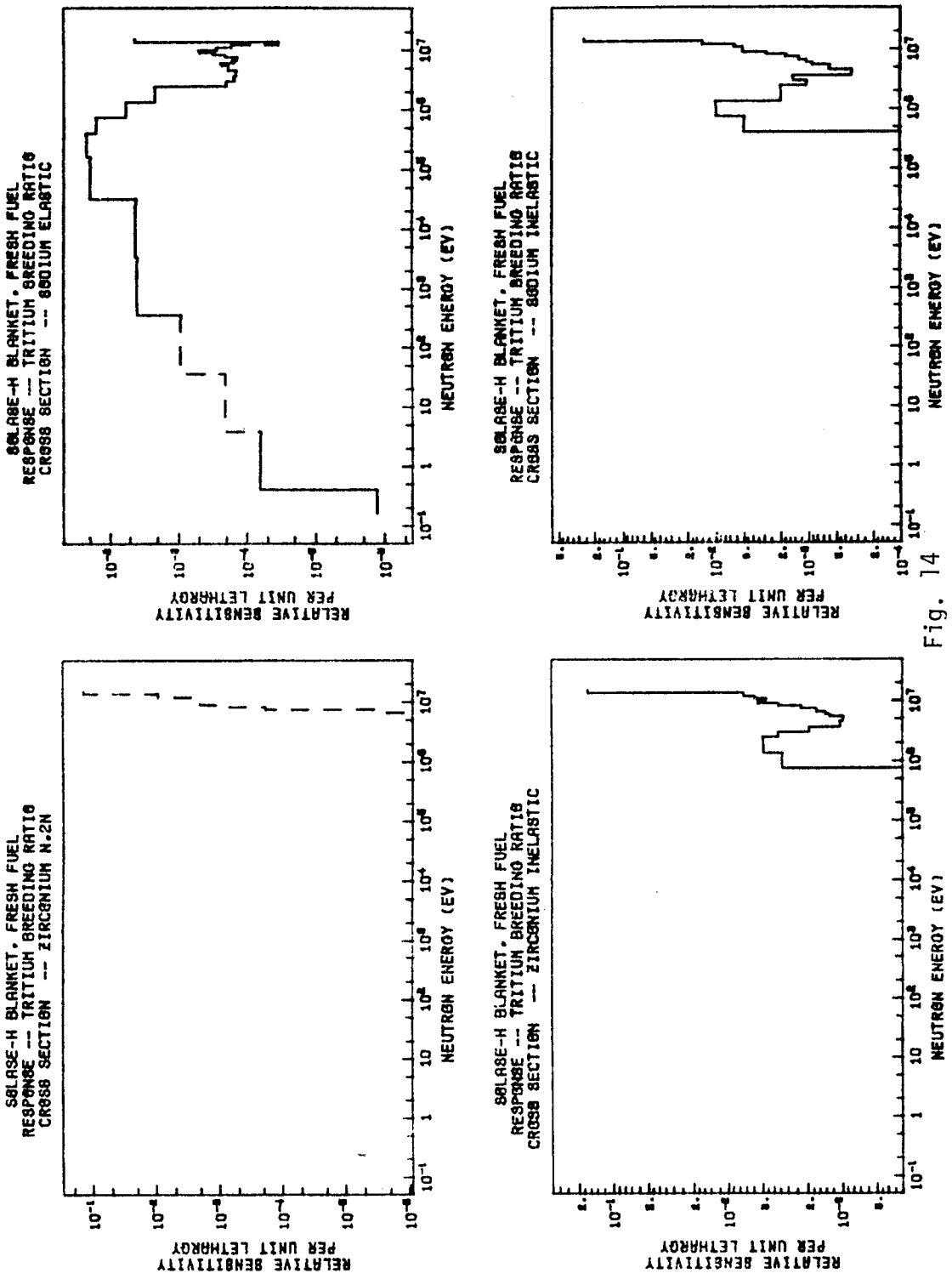
SOLASE-H BLANKET, FRESH FUEL
RESPONSE -- TRITIUM BREEDING RATIO
CROSS SECTION -- SODIUM ELASTIC
SOLASE-H BLANKET, FRESH FUEL
RESPONSE -- TRITIUM BREEDING RATIO
CROSS SECTION -- SODIUM INELASTIC
SOLASE-H BLANKET, FRESH FUEL
RESPONSE -- TRITIUM BREEDING RATIO
CROSS SECTION -- ZIRCONIUM N,2N
SOLASE-H BLANKET, FRESH FUEL
RESPONSE -- TRITIUM BREEDING RATIO
CROSS SECTION -- ZIRCONIUM INELASTIC
RELATIVE SENSITIVITY PER UNIT LETHARGY
NEUTRON ENERGY (EV)

Fig. 14

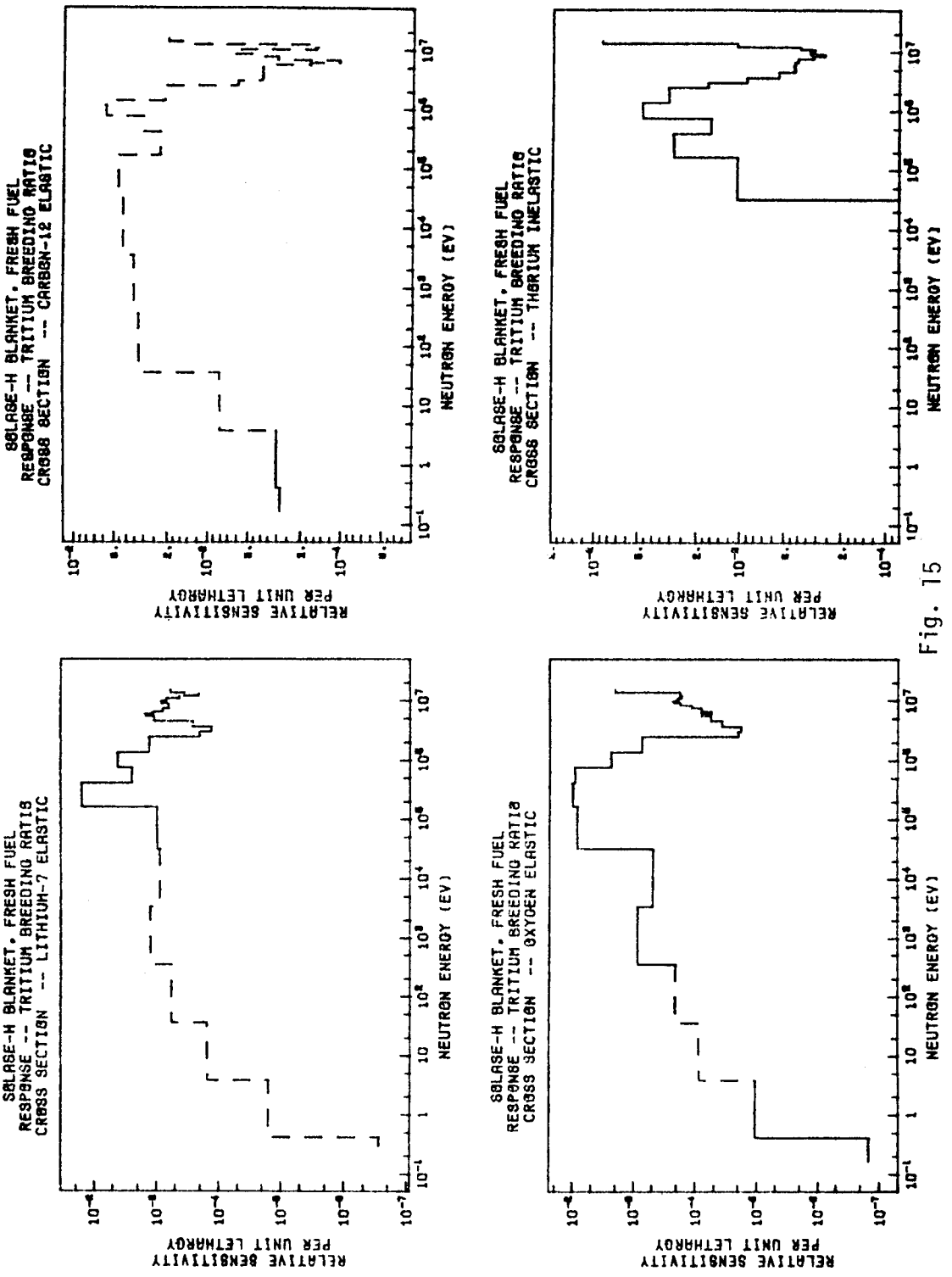
SOLASE-H BLANKET, FRESH FUEL
RESPONSE -- TRITIUM BREEDING RATIO
CROSS SECTION -- CARBON-12 ELASTIC
SOLASE-H BLANKET, FRESH FUEL
RESPONSE -- TRITIUM BREEDING RATIO
CROSS SECTION -- THORIUM INELASTIC
SOLASE-H BLANKET, FRESH FUEL
RESPONSE -- TRITIUM BREEDING RATIO
CROSS SECTION -- LITHIUM-7 ELASTIC
SOLASE-H BLANKET, FRESH FUEL
RESPONSE -- TRITIUM BREEDING RATIO
CROSS SECTION -- OXYGEN ELASTIC
RELATIVE SENSITIVITY PER UNIT LETHARGY
NEUTRON ENERGY (EV)

Fig. 15

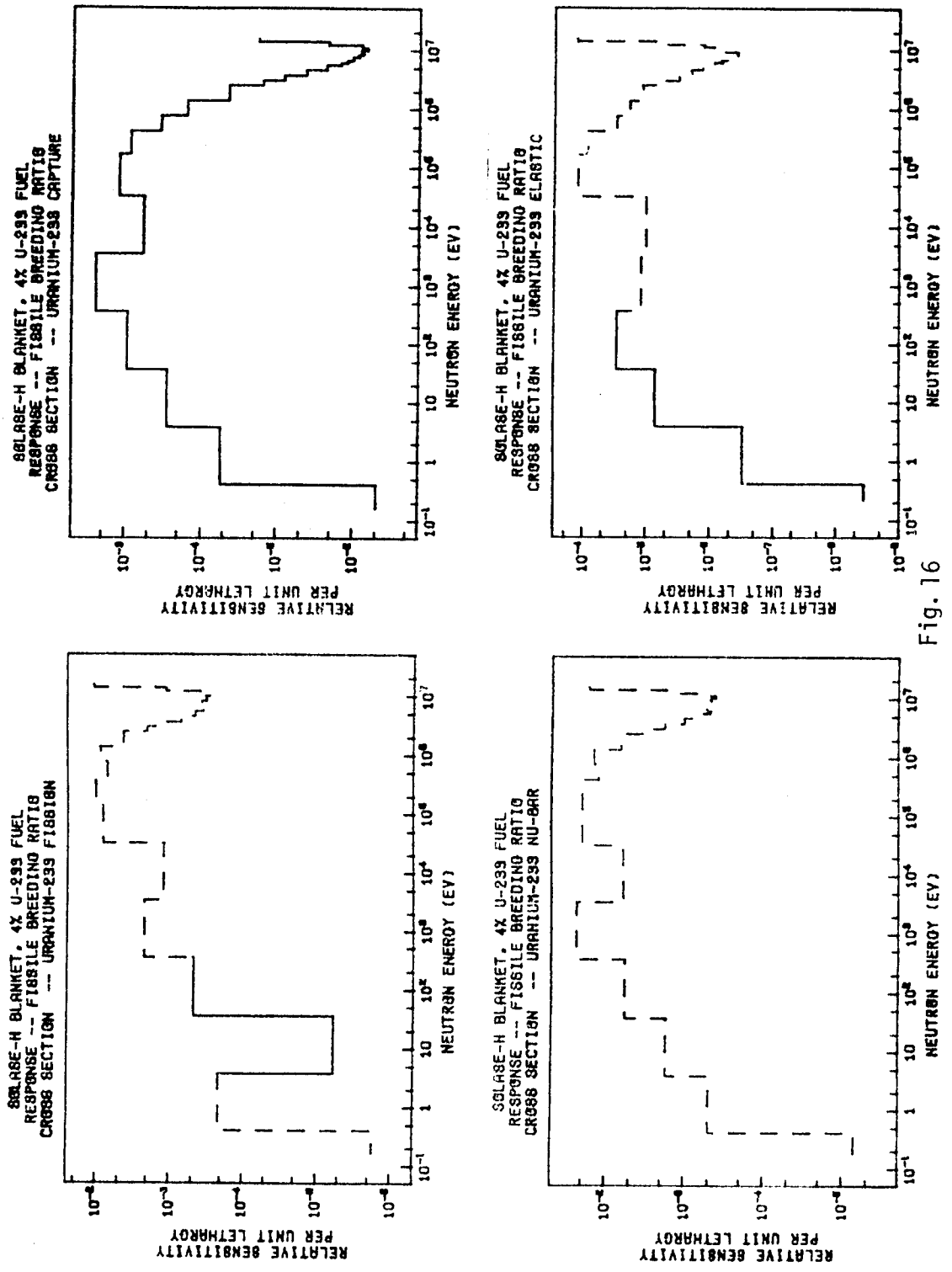
SOLASE-H BLANKET, 4% U-233 FUEL
RESPONSE -- FISSILE BREEDING RATIO
CROSS SECTION -- URANIUM-238 CAPTURE
SOLASE-H BLANKET, 4% U-233 FUEL
RESPONSE -- FISSILE BREEDING RATIO
CROSS SECTION -- URANIUM-233 ELASTIC
SOLASE-H BLANKET, 4% U-233 FUEL
RESPONSE -- FISSILE BREEDING RATIO
CROSS SECTION -- URANIUM-233 FISSION
SOLASE-H BLANKET, 4% U-233 FUEL
RESPONSE -- FISSILE BREEDING RATIO
CROSS SECTION -- URANIUM-233 NU-BAR
RELATIVE SENSITIVITY PER UNIT LETHARGY
NEUTRON ENERGY (EV)

Fig. 16

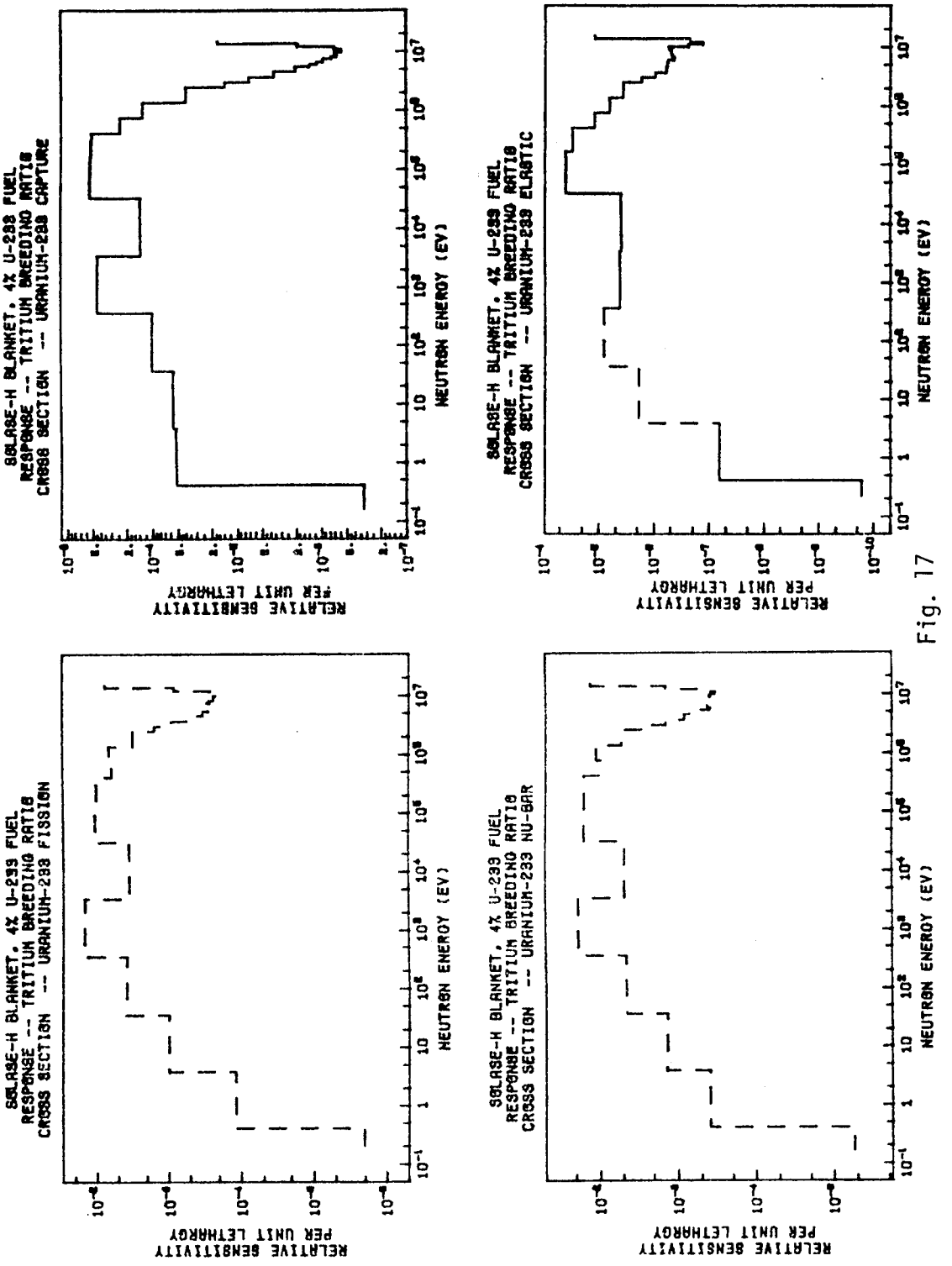
SOLASE-H BLANKET, 4% U-233 FUEL
RESPONSE -- TRITIUM BREEDING RATIO
CROSS SECTION -- URANIUM-238 CAPTURE
SOLASE-H BLANKET, 4% U-233 FUEL
RESPONSE -- TRITIUM BREEDING RATIO
CROSS SECTION -- URANIUM-238 ELASTIC
SOLASE-H BLANKET, 4% U-233 FUEL
RESPONSE -- TRITIUM BREEDING RATIO
CROSS SECTION -- URANIUM-238 FISSION
SOLASE-H BLANKET, 4% U-233 FUEL
RESPONSE -- TRITIUM BREEDING RATIO
CROSS SECTION -- URANIUM-233 NU-BAR
RELATIVE SENSITIVITY PER UNIT LETHARGY
NEUTRON ENERGY (EV)

Fig. 17

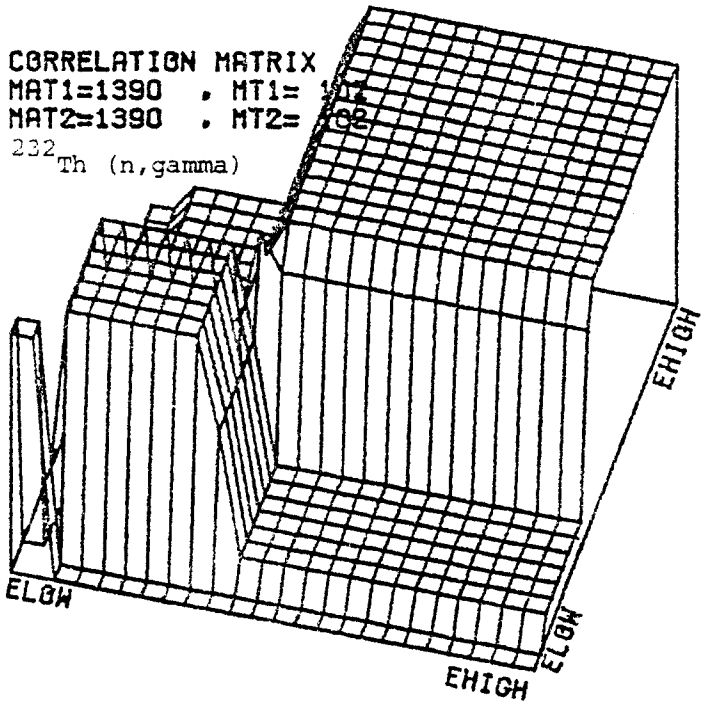
CORRELATION MATRIX
MAT1=1390 . MT1=
MAT2=1390 . MT2=
232Th (n,gamma)
ELOW
EHIGH
ELOW
EHIGH

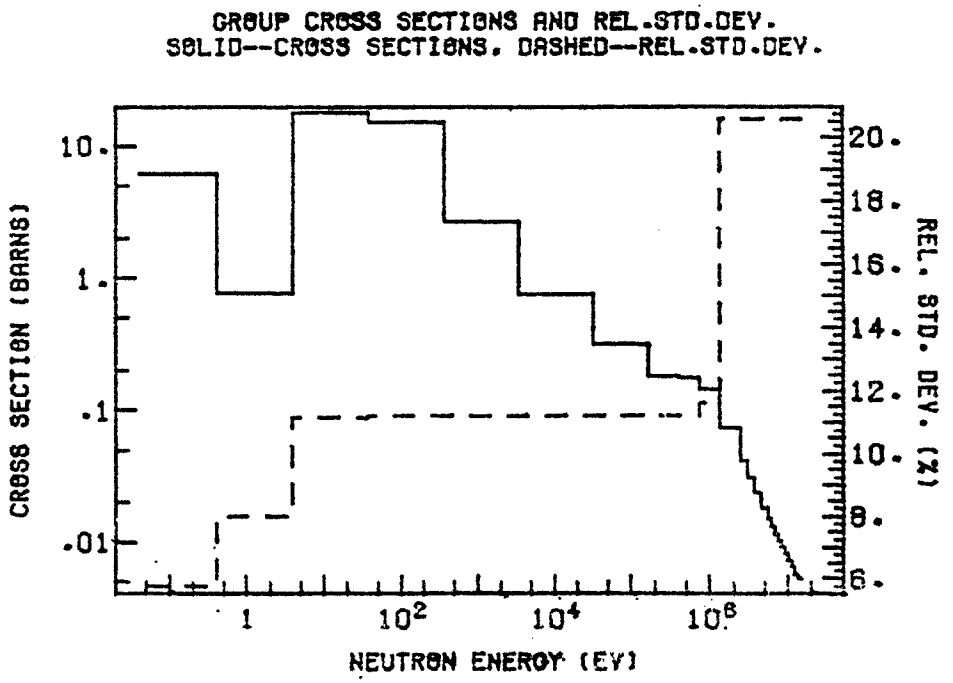
GROUP CROSS SECTIONS AND REL.STD.DEV.
SOLID--CROSS SECTIONS, DASHED--REL.STD.DEV.
CROSS SECTION (BARNS)
10.
1.
.1
.01
1
10²
10⁴
10⁶
NEUTRON ENERGY (EV)
REL. STD. DEV. (%)
20.
18.
16.
14.
12.
10.
8.
6.

Fig. 18

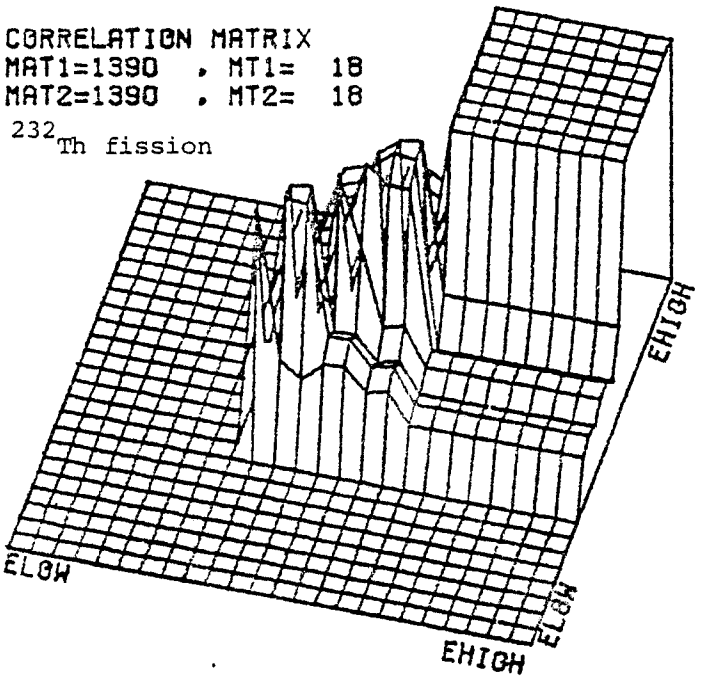
CORRELATION MATRIX
MAT1=1390 , MT1= 18
MAT2=1390 , MT2= 18
232Th fission
ELOW
EHIGH
ELOW
EHIGH

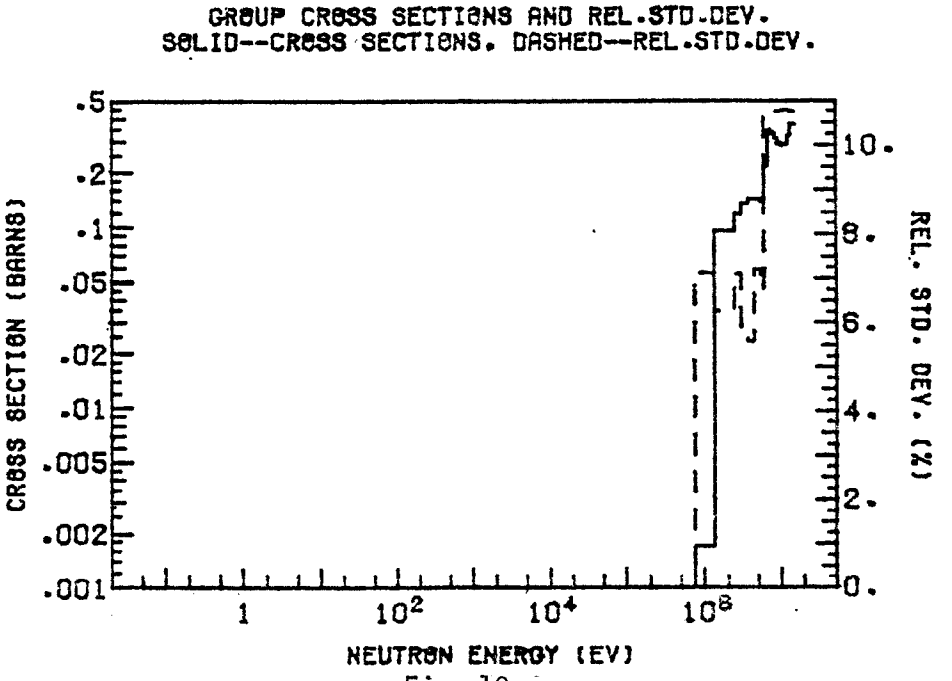
GROUP CROSS SECTIONS AND REL.STD.DEV.
SOLID--CROSS SECTIONS, DASHED--REL.STD.DEV.
CROSS SECTION (BARNS)
.5
.2
.1
.05
.02
.01
.005
.002
.001
1
10²
10⁴
10⁸
NEUTRON ENERGY (EV)
REL. STD. DEV. (%)
10.
8.
6.
4.
2.
0.

Fig. 19

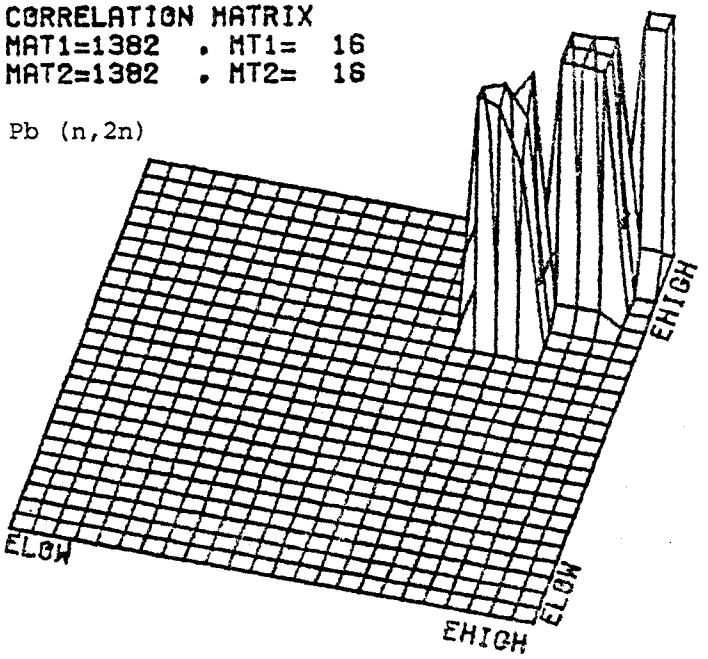
CORRELATION MATRIX
MAT1=1382 . MT1= 16
MAT2=1382 . MT2= 16
Pb (n,2n)
ELOW
EHIGH
ELOW
EHIGH

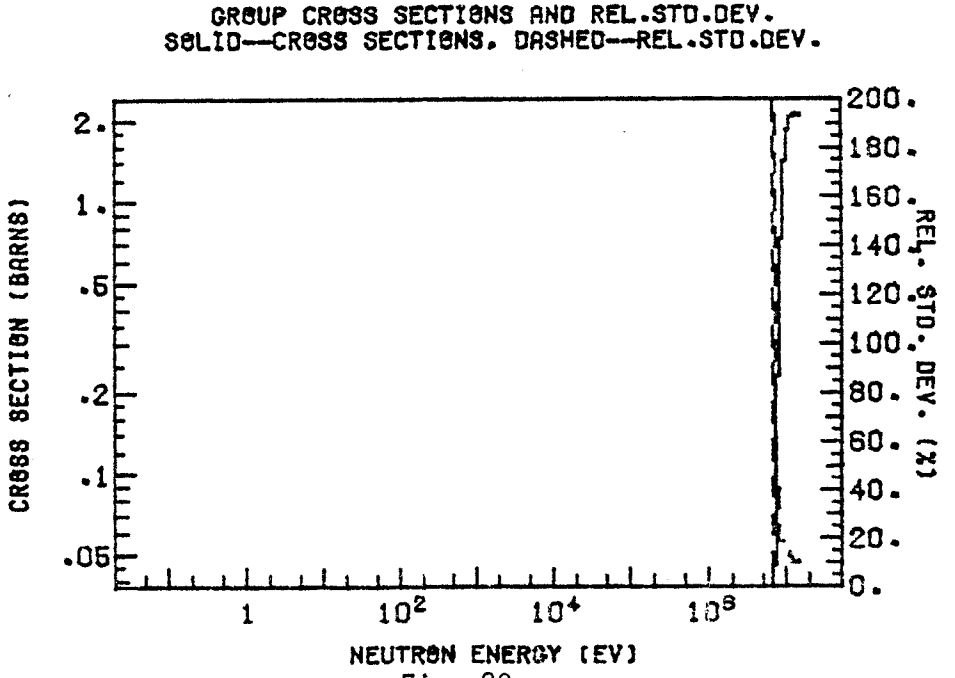
GROUP CROSS SECTIONS AND REL.STD.DEV.
SOLID—CROSS SECTIONS, DASHED—REL.STD.DEV.
CROSS SECTION (BARNS)
2.
1.
.5
.2
.1
.05
200.
180.
160.
140.
120.
100.
80.
60.
40.
20.
0.
REL. STD. DEV. (%)
1
10²
10⁴
10⁶
NEUTRON ENERGY (EV)

Fig. 20

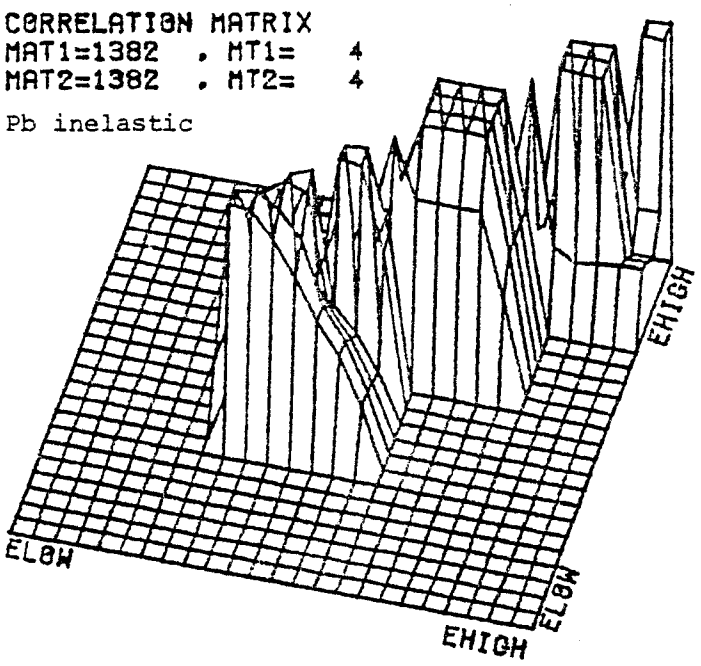
CORRELATION MATRIX
MAT1=1382 , MT1= 4
MAT2=1382 , MT2= 4
Pb inelastic
ELOW
EHIGH
ELOW
EHIGH

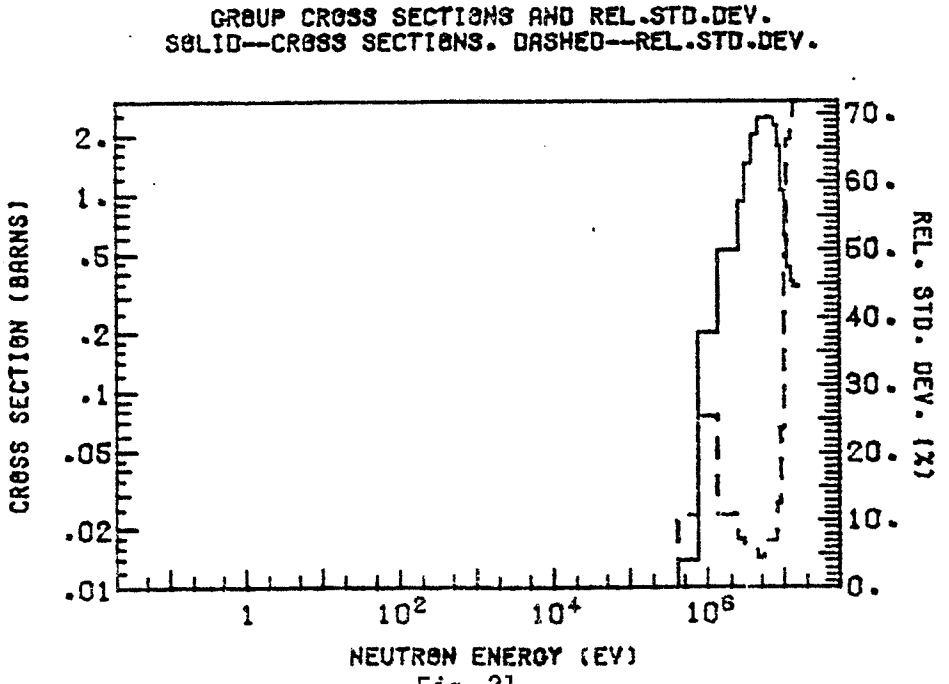
GROUP CROSS SECTIONS AND REL.STD.DEV.
SOLID--CROSS SECTIONS. DASHED--REL.STD.DEV.
CROSS SECTION (BARNS)
2.
1.
.5
.2
.1
.05
.02
.01
1
10^2
10^4
10^6
NEUTRON ENERGY (EV)
REL. STD. DEV. (%)
70.
60.
50.
40.
30.
20.
10.
0.

Fig. 21

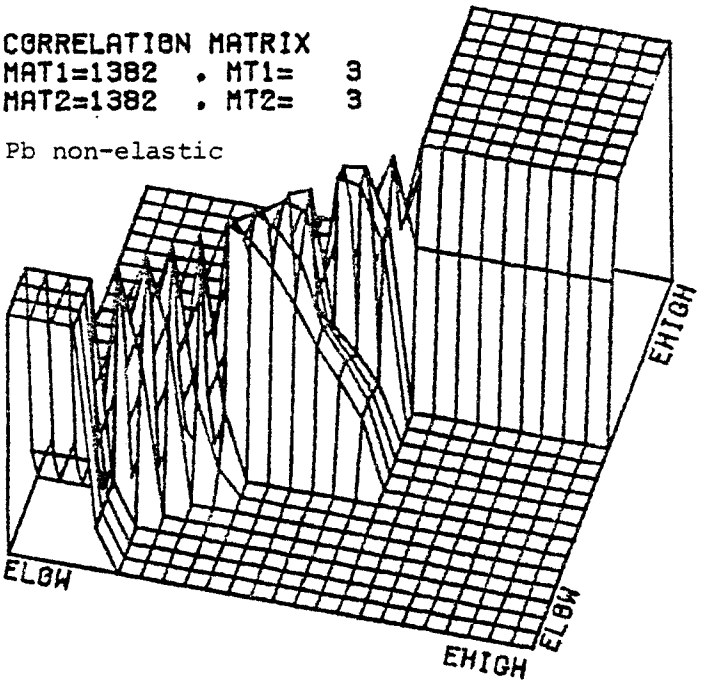

GROUP CROSS SECTIONS AND REL.STD.DEV.
SOLID—CROSS SECTIONS. DASHED—REL.STD.DEV.

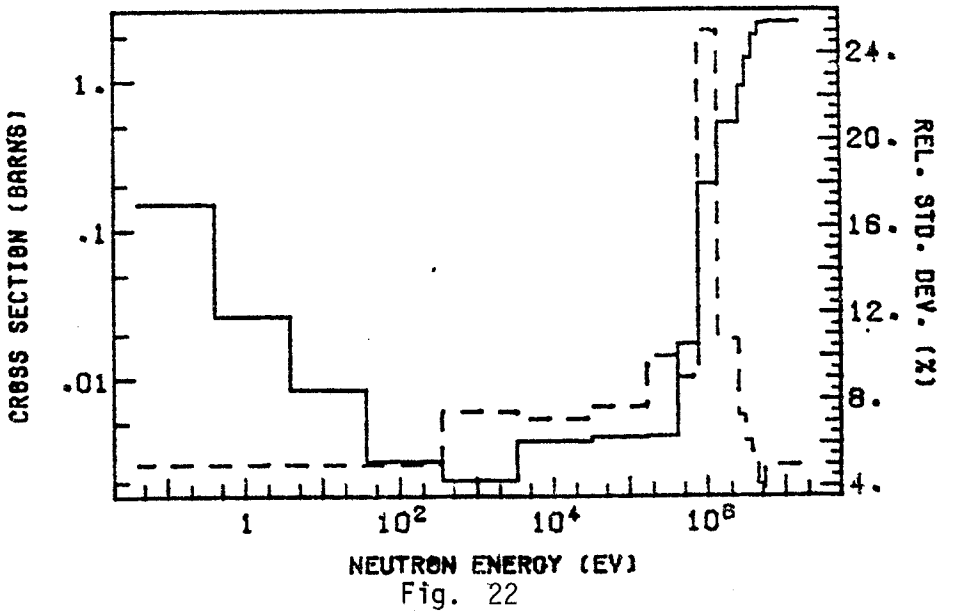

Fig. 22

CORRELATION MATRIX
MAT1=1382 , MT1= 4
MAT2=1382 , MT2= 3

Pb inelastic vs. non-elastic

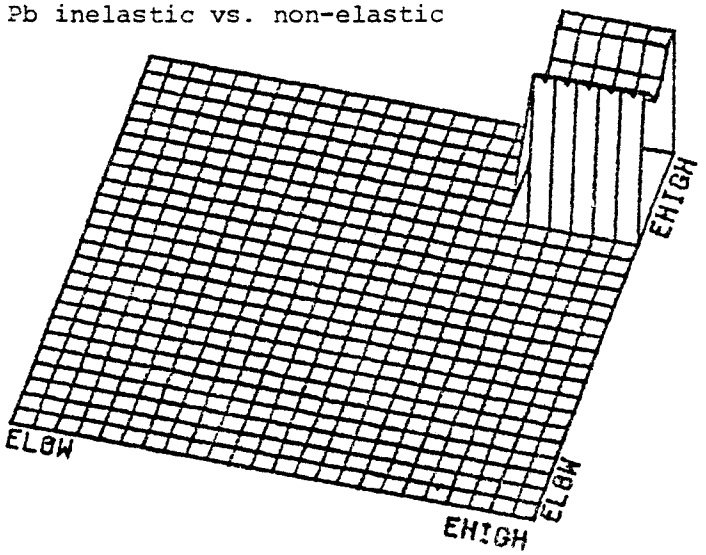

CORRELATION MATRIX
MAT1=1382 , MT1= 4
MAT2=1382 , MT2= 16

Pb inelastic vs. (n,2n)

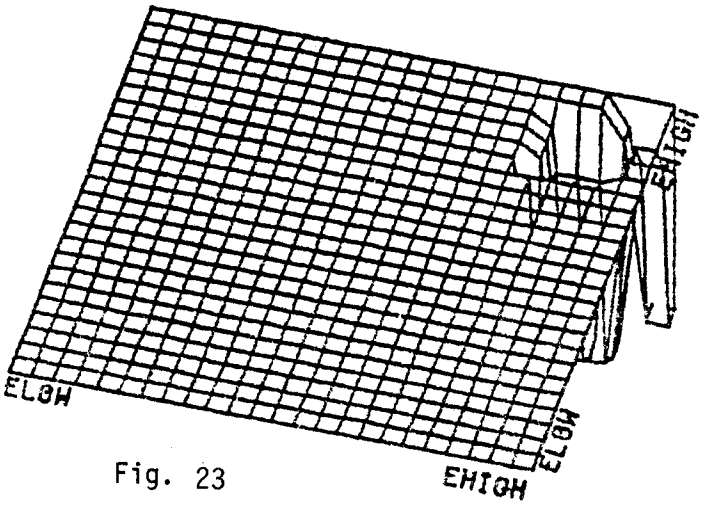

Fig. 23

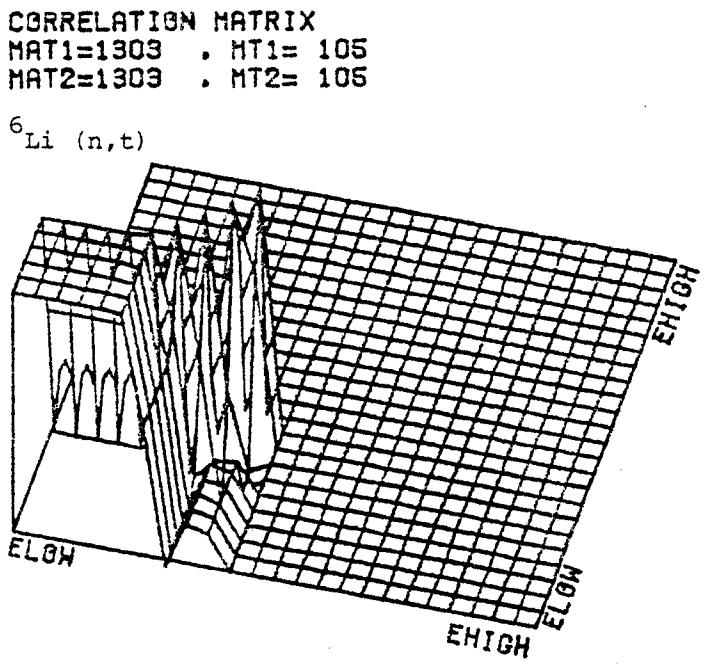
CORRELATION MATRIX
MAT1=1303 . MT1= 105
MAT2=1303 . MT2= 105
^{6}Li (n,t)
ELOW
EHIGH
ELOW
EHIGH

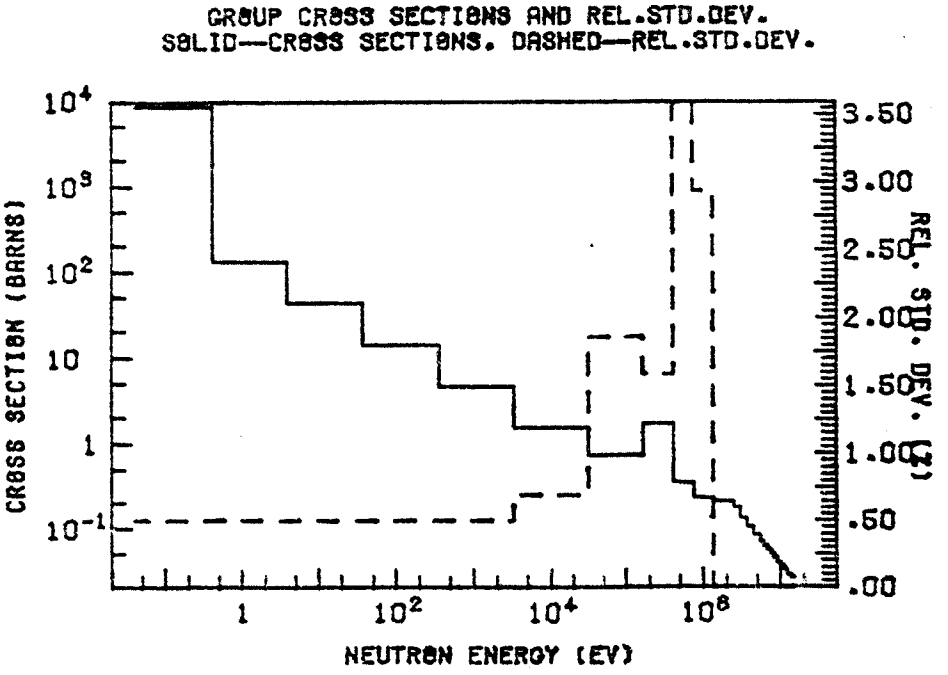
GROUP CROSS SECTIONS AND REL.STD.DEV.
SOLID—CROSS SECTIONS. DASHED—REL.STD.DEV.
CROSS SECTION (BARNS)
REL. STD. DEV. (%)
NEUTRON ENERGY (EV)

Fig. 24

APPENDIX

A Modified Sensitivity Code: SWANLAKE-UW

The sensitivity code, SWANLAKE[1], has been used extensively for calculating the sensitivity coefficients of the responses with respect to the microscopic cross section data in the field of the fusion reactor blanket and shield design. There are, however, some notable limitations which restrict the applicability of this code. For example: (1) It cannot evaluate the sensitivity of the response to the response function - the direct effect term. Therefore, one has to compute the indirect effect via SWANLAKE and the direct effect through other numerical programs in order to obtain the total sensitivity which is the quantity used in data uncertainty analysis. (2) It does not include the effect of the fission cross sections. Thus, this code is not applicable to the fusion-fission hybrid system where the effects of the fission cross sections may not be negligible. For the purpose of investigating the sensitivity of the responses to the basic nuclear data in a hybrid system, we have successfully modified the SWANLAKE code such that the afore-mentioned deficiencies can be remedied in addition to some other minor changes.

The relative sensitivity function, $S(r,E)$, of a response R with respect to a cross section $\Sigma(r,E)$ at energy E and position r,

can be derived from the basic definition $S = (\Sigma/R)\ (\partial R/\partial \Sigma)$ and the result from the first-order perturbation theory, i.e.,

$$\delta R \simeq \langle \phi^*, \delta\Sigma_r \rangle - \langle \phi\ , \delta L^+ \phi^*\ \rangle ,$$

where

ϕ, ϕ^* = forward and adjoint anuglar fluxes,

L^+ = adjoint transport operator,

Σ_r = response function which is also the adjoint source for the adjoint equation,

and $\langle\ ,\ \rangle$ represents the integration over the phase space. Therefore, $S(r,E)$ can be expressed as the sum of four terms. That is,

$$S(r,E) = S_{de}(r,E) + S_{fg}(r,E) + S_{cl}(r,E) + S_{sg}(r,E),$$

where

$S_{de}(r,E)$ = detector term (direct effect)

$$= \frac{\partial \Sigma_r(r,E)}{\partial \Sigma\ (r,E)}\ \Sigma(r,E) \int d\Omega \phi(r,E,\Omega)/R\ ,$$

$S_{fg}(r,E)$ = fission gain term

$$= \nu(E)\Sigma_f(r,E)\{\int d\Omega \phi(r,E,\Omega)\} \iint dE' d\Omega' \chi(E') \phi^* (r,E',\Omega')/R\ ,$$

$S_{sg}(r,E)$ = scattering gain term

$$= \sum_{\ell} \frac{2\ell+1}{4\pi} \int dE' \{ \left[\int d\Omega P_{\ell}(\Omega) \phi(r,E,\Omega) \right] \sum_{\ell}^{s} (E \to E') \left[\int d\Omega' P_{\ell}(\Omega') \phi^{*}(r,E',\Omega') \right] \} / R ,$$

$S_{cl}(r,E)$ = collision loss term

$$= -\Sigma(r,E) \int d\Omega \phi^{*}(r,E,\Omega) \phi(r,E,\Omega)/R \quad .$$

Note that the direct effect term exists only if (1) Σ is the response function itself or, (2) any change in Σ will affect the response function (for instance, if $^{6}Li(n,t)$ is the cross section of interest while the response is total tritium production). It is the fission gain term that accounts for the effect of fission cross sections of the fissionable nuclides in a hybrid system.

In this modified sensitivity code we have chosen to use an output logical unit to store the relevant data generated by the code in a fashion that it would be easier to extract the information needed for further uncertainty analysis or for plotting the sensitivity profiles. The input instruction and output description will be discussed as follows.

Input Instruction

Either conventional FIDO ($ or *) or free-form ($$ or **) format may be used for input data in the order listed. The bracketed numbers refer to the number of entries required for each unit. Also a brief explanation will be included with each input item.

1$ [16]

(1)	IGM	number of energy groups
(2)	ITL	cross section table length (IGM+3 or larger)
(3)	INT	number of spatial intervals
(4)	ISN	order of S_N
(5)	ISCT	order of cross section expansion
(6)	NZONE	number of spatial zones
(7)	NE	number of cross section sets
(8)	ITAPE	1/2 - $\phi^*\phi$ matrix to be calculated/read from unit 7
(9)	ISIG	1/2 - cross sections from cards/tape
(10)	IGOM	1/2/3 - plane/cylinder/sphere geometry
(11)	IPRNT	0/1 - do not/print cross sections
(12)	IPLZN	(not used)
(13)	IARNG	(not used)
(14)	IPLOT	(not used)
(15)	IPLTZ	(not used)
(16)	ILNG	last neutron group

2* [1]

RTOTAL integrated response, R, for the problem investigated

T

The following data (4*,5*,6* and 7$) are required only if ITAPE=1

4*[NOA]†	S_n weights
5*[NOA]	S_n cosines
6*[INT+1]	interval boundaries (cm)
7$[NZONE+1]	numbers of interval boundaries corresponding to zone boundaries

T

8*[ILNG]	neutron energy group boundaries in MeV, high to low
9*[IGM-ILNG+1]	gamma energy group boundaries in MeV, high to low

T

The following data (title card, 10$, 11* or 11$, 12*, and 13* or 13$) must be repeated for each cross section set to be analyzed (INE=1 to NE)

Title card (20A4) for cross section set INE

10 $ [2] LISN,IDRT

† NOA = ISN+1 for plane or sphere
NOA=(ISN(ISN+4))/4 for cylinder

LISN $\geq$ 0 order of P_L for cross section set INE

LISN < 0 cross section set INE is a non-scattering process:

= -5 to be read from cards (11*)

= -8 to be read from tape (11$)

= -18 to be read from tape (11$) and sensitivity includes fission gain.

IDRT = 0 no direct effect

= 5/8 response function to be read from cards (13*)/tape (13$)

T

11* [IGM*ITL*(LISN+1)]

cross section set INE input on cards (ISIG=1 and LISN $\geq$ 0)

or

11$ [LISN+1] library ID numbers for cross section set INE to be inputed from unit 8 (ISIG=2 and LISN $\geq$ 0)

or

11$ [2] IID,IPOS

library ID number (IID) and position (IPOS) for cross section set INE to be input from unit 8 (LISN=-8 or -18)

T

12*[NZONE]	nuclide density by zone for cross section set INE
T	
13*[IGM]	response function (IDRT=5)
or	
13$[2]	IDD,IPOSD library ID number (IDD) and position (IPOSD) for detector response function (IDRT=8)
T	

Output Description

Logical unit 11 is assigned to store the sensitivities generated by this code for further sensitivity and uncertainty analysis. The structure of unit 11 is as follows:

Record 1 (415) IGM, IGMM, NZONE, NE

IGM	=	total number of energy groups
IGMM	=	IGM+1 (neutron only) or IGM+2
NZONE	=	number of spatial zones
NE	=	number of cross section sets.

Record 2 to 6 will be repeated for each cross section set (INE=1 to NE).

Record 2 (A3,I3) DUM,INE (DUM=3HSET)

Record 3 (20A4) Title card for cross section set INE

Record 4 (I2,A1) INE,AA (AA=1H*)

Record 5 (FIDO format)

Relative sensitivity matrix

SEN(I,J,K),I=1 to IGMM, J=1 to NZ1, K=1 to 6,

where

I=1 to IGM: sensitivity coefficient for group I

=IGM+1 : sum over all neutron groups

=IGM+2 : sum over all photon groups (if exists)

J=1 to NZONE : sensitivity for spatial zone J

=NZ1 (NZONE+1) : sum over all spatial zones

K=1 direct effect

=2 fission gain

=3 collision loss

=4 scattering loss

=5 total indirect effect (2+3+4)

=6 net effect (1+5)

Record 6 (2X,A1) TT (TT=1HT)

Reference

1. D.E. Bartine, E.M. Oblow, and F.R. Mynatt, "SWANLAKE--A Computer Code Utilizing ANISN Radiation Transport Calculations for Cross Section Sensitivity Analysis," ORNL/TM-3809, Oak Ridge National Laboratory (1973).